A novel molecule in the Ras signaling pathway, Flightless-1 (FLI-1), affects germ line morphogenesis, muscle development and germ line tumor formation in *C. elegans*

by

Jiamiao Lu

Submitted to the Department of Molecular Biosciences

and the Faculty of the Graduate School of the University of Kansas

in Partial Fulfillment of the Requirements for the Degree of

Doctor of Philosophy

_____

Erik Lundquist, Ph. D., Chairperson

_____

Lisa Timmons, Ph. D.

_____

Robert Cohen, Ph. D.

Date submitted: _____

The Dissertation Commmittee for Jiamiao Lu certifies that this is the approved version of the following dissertation:

A novel molecule in the Ras signaling pathway, Flightless-1 (FLI-1), affects germ line morphogenesis, muscle development and germ line tumor formation in *C. elegans*

Committee:

_____
Erik Lundquist, Ph. D., Chairperson

Date approved:_____

ABSTRACT
Jiamiao Lu, Ph. D.
Department of Molecular Biosciences, April 2007
University of Kansas

The wild-type *C. elegans* germ line is a syncytium with multiple nuclei sharing a common cytoplasm. At the distal tips, germ cell nuclei are mitotic and have stem cell character. As the syncytial nuclei move proximally, they enter meiosis and become arranged at the germ cell plasma membrane, forming a single layer of nuclei around the nucleus-free center (the rachis). Fingers of germ cell plasma membrane invaginate around the nuclei but do not completely enclose them. In *fli-1* mutants, chains of meiotic germ line nuclei were present in the central rachis. Germ cell plasma membrane and the overlying sheath cell, which normally invaginates into the spaces between germ nuclei, remained associated with the misplaced meiotic nuclei, suggesting excessive invagination of the germ cell plasma membrane and sheath cell. This arrangement is reminiscent of the normal distal tip region, suggesting that *fli-1* might control the morphogenetic rearrangement of nuclei accompanying entry into meiosis. A rescuing full-length *fli-1::gfp* reporter gene was expressed in the germ line, and FLI-1::GFP associated with germ line nuclei.

To dissect molecular mechanisms of FLI-1 activity in the germ line, interactions of *fli-1* with other mutations affecting germ line development were analyzed. Loss-of-function and dominant-negative mutations in the *let-60* Ras and other Ras pathway components also caused this germ cell phenotype. Constitutively-active LET-60 Ras partially rescued the germ cell defect in both *fli-*

1 alleles, suggesting that FLI-1 and LET-60 Ras control germ cell morphogenesis together. While *fli-1* alone caused no defects in mitotic or meiotic differentiation, preliminary results indicate *fli-1(ky535)* partially suppressed the germ cell tumor phenotype of *gld-1(q485)*. In *gld-1(q485),* germ cells re-enter mitosis after beginning meiotic differentiation and proliferate until they fill the gonad and eventually the body cavity, killing the animal. *fli-1(ky535);gld-1(q485)* animals survived slightly longer than *gld-1* alone, and staged animals displayed fewer and larger tumorous germ cells. Experiments are underway to determine how *fli-1* mutation suppresses *gld-1*, but initial analyses indicate that *fli-1* might delay re-entry into mitosis.

Drosophila flightless 1 mutants display disorganized indirect flight muscle structure. We found that FLI-1 also controls muscle development in *C. elegans*. In *fli-1(ky535)* mutants, disorganized body wall muscle myofilament structure was observed by both TEM and birefringence. The *fli-1(tm362)* caused Pat phenotype (Paralyzed Arrested at Two fold stage), suggesting severe body wall muscle defects.

Acknowledgements

This thesis is the last step of my long journey in obtaining my Ph.D. degree in Molecular Biosciences. The writing of this thesis itself is a time-consuming and stressful procedure. Obviously, this work would not have been possible without the encouragement and practical support of numerous people. I would like to express my deep and sincere gratitude to all those who helped me, encouraged me and gave me the possibility to finish my Ph.D. education and this thesis.

I want to express my sincere thanks to my Ph.D. advisor, Professor Erik Lundquist, who introduced me to the field of *C. elegans* and genetics, trained me to do scientific research, inspired me with brilliant ideas and encouraged me to pursue a career in science. The knowledge I have learned from him will have a remarkable influence on my entire life.

I wish to thank my committee members, Professor Lisa Timmons, Professor Robert Cohen, Professor Victoria Corbin, Professor Erik Floor and Professor Jennifer Gleason, for their interesting discussions and valuable advices about my research work, especially to Professor Lisa Timmons and her laboratory for giving me reagents and animal strains generously.

My research work for this thesis was made more efficiently by using the Transmission Electron Microscope. Thus my thanks go out to Professor William Dentler, who trained me to do TEM patiently.

I also would like to thank Professor David Hall, Professor David

Greenstein, Professor Tim Schedl and Professor Judith Kimble, who generously shared their reagents, protocols, and ideas with me.

My graduate life would not be the same without the help from John Patrick Connolly, the Graduate Program Assistant of the Division of Biological Sciences. I would like to thank him for helping me to arrange every committee meeting even my final defense and for making my life easier here as an international student.

I cannot end without expressing my thanks to my family members, my mother Keyi Zhang, my father Jianxiong Lu and my husband Qian Ma, on whose love and encouragement I have relied throughout my graduate study.

Table of Contents

List of Figures

Chapter I: **Introduction**

Chapter II: **The actin-binding protein FLI-1 flightless-1 acts with LET-60 Ras to control germ line morphogenesis in *C. elegans***

CHAPTER I

INTRODUCTION

Evolution and natural selection are the keys to understand biological diversity. Meanwhile, from bacteria to human, many essential genes and their functions in basic life processes are extraordinarily conserved. Because of the high degree of conservation of basic developmental processes, genes in the less complex organisms often encode proteins that have similar structures and functions as their homologous counterparts in more complex organisms, such as human. For this reason and due to the difficulties to perform experiments in human, model organisms are valuable tools for scientists to explore the nature of life and various diseases. Since Sydney Brenner chose *Caenorhabditis elegans* as a promising model animal for biological research in 1965, extensive studies performed in this key model organism have identified numerous genes with essential functions in development. Here we present the studies we have done on a *C. elegans flightless-1* (*fli-1)* gene (encodes a homolog of human protein FLI1) and its regulatory functions in germ line and muscles.

Mutations in *flightless 1* were first isolated in another model organism, *Drosophila melanogaster*. Flies carrying loss-of-function mutations of *flightless 1* are viable but loss the ability to fly (Homyk, T. et al. 1977, Koana, T. et al. 1978 and Deak, I.I. et al. 1980). Ultrastructural analysis of these alleles detected disorganized myofibrils in the indirect flight muscles but not the direct flight muscles (Koana, T. et al. 1978, Deak, I.I. et al. 1982 and Miklos, G.L.G. 1990). Severe *flightless 1* mutant *Drosophila* embryos do not cellularize completely and gastrulate abnormally (Straub, K.L. et al 1996). In these embryos, the syncytial blastoderm nuclei first migrate to the cortex of the egg normally, but during cellularisation, these nuclei loss the ability to maintain cortical positioning. Since

cellularisation is incomplete, these nuclei are only partially covered by the membrane. When these nuclei loss cortical positioning, they drop from the cortex and some even migrate to the center of the egg. *Drosophila flightless 1* encodes a protein that consists 1256 amino acid residues, with a N-terminus containing leucine-rich-repeat (LRR) sequences, and a C-terminus containing gelsolin related structures that bind with actin.

Human FLI1 protein is 58% identity to *Drosophila* FLI1 at the amino acid sequence level (Campbell, H.D. et al. 1993). Human FLI1, along with a monomer of G-actin, is a component of a transcriptional coactivator complex that acts with nuclear hormone receptors. Multiple mapping experiments showed that human *FLI1* is located on chromosome 17, 17p11.2, which is a region been deleted in Smith-Magenis syndrome (SMS) (Campbell, H.D. et al. 1997 and Chen, K.S. et al. 1995). SMS is a developmental disorder that affects 1 in every 25,000 human individuals and characterized by distinctive facial features, developmental delay, REM sleep abnormalities, and behavioral problems. Individuals having SMS exhibit from mild to moderate range of mental retardation (Smith, A.C. et al. 1986 and Greenberg, F. et al. 1996). SMS is thought to be a contiguous-gene deletion syndrome associated with an interstitial deletion of the short arm of chromosome 17 in band p11.2. Deletions of 2Mb to 10Mb are usually detected on chromosomal region 17p11.2 of SMS patients (Trask, B.J. et al. 1996). It seems likely that genes deleted in this region are responsible for SMS.

Deletions of the short arm of chromosome 17 are also commonly found in patients with childhood Primitive Neuroectodermal Tumors (PNETs) of the medulloblastoma. This deletion region is partially overlapped with the deletion

interval found in SMS (including *FLI1* region), raising the possibility that genes located within this region are tumor suppressors (Seranski, P. et al. 1999, Scheurlen, W.G. et al. 1997 and Wilgenbus, K.K. et al. 1997). Gelsolin itself is implicated as a candidate tumor suppressor (Kwiatkowski, D.J. et al. 1999, Tanaka, M. et al. 1999 and Asch, H.L. et al. 1996). Possibly, gelsolin-related genes might also have tumor suppression functions. As a gelsolin repeat containing protein, FLI1 may function as a tumor suppressor.

A highly conserved homologue of *flightless 1* is also present in *C. elegans* (49% identical with *Drosophila* FLI1 at the amino acid sequence level) (Campbell, H.D. et al. 1993). The *C. elegans* FLI-1 protein is comprised of 1257 amino acid residues with a N-terminus containing 17-fold leucin-rich repeats (LRR) and a C-terminus containing 5 gelsolin repeats. LRR domains of human FLI1 and *C. elegans* FLI-1 exhibit 54% identity and 73% similarity at the amino acid sequence level. LRRs are involved in protein-protein interactions. Evidence presented by Goshima M. et al. indicated that the N-terminal 770 amino acids of *C. elegans* FLI-1 that contains LRR could bind specifically with human Ha-Ras. Other Ras-related proteins such as Rho, Rac and CDC42 could not interact with *C. elegans* FLI-1 LRR directly (Goshima, M. et al. 1999). Human and *C. elegans* Ras also exhibit high level of conservation, such as *C. elegans* RAS-2 and human N-ras are 41% identical and 57% similar at the amino acid sequence level. The gelsolin repeats of *C. elegans* FLI-1 can bind to and sever actin filaments.

By using human FLI1 LRR as bait, Liu and Yin identified a novel protein that interacts with FLI1 LRR through yeast two-hybrid system. This protein is called FLAP for FLI1 LRR associated protein (Liu, Y.T. et al. 1998). *C. elegans*

gene F57B9.7 encodes a homologue of *FLAP. C. elegans* FLAP protein has RNA-binding activity and contains potential nuclear localization signals.

Since *C. elegans* FLI-1 and human FLI1 are highly conserved, the studies done in *C. elegans fli-1* will provide us detailed knowledge about human FLI1 functions. Here we describe the discovery and characterization of a novel *C. elegans* germ line phenotype caused by loss of *fli-1* activity and the possibility that *fli-1* as a novel factor in Ras signaling pathway to coordinate germ line nuclei meiotic differentiation with rachis morphogenesis.

Each hermaphrodite *C. elegans* germ line contains two gonad arms. The distal half of the gonad is a syncytium, with multiple germ line nuclei sharing the common cytoplasm and membrane structures. Fully differentiated germ line nuclei are generated by germ line stem cells reside at the distal tip of each gonad arm. Distal tip cell (DTC) that function as the stem cell niche covers the distal tip part of the gonad and interacts with germ line stem cells by extending projections into the interior region of the gonad. This interaction of DTC maintains the stem cell fate (the mitotic zone) of the germ line stem cells. Germ line stem cells proliferate to renew themselves and generate differentiated germ line nuclei, which will move from the distal tip to the proximal part of the gonad. As the nuclei proceed proximally, they lose their mitotic character and enter meiosis (the transition zone). Moving out of the transition zone, all nuclei enter the pachytene stage of meiosis. Meanwhile, the meiotic nuclei migrate to the peripheral cortex of the gonad leaving a nucleus-free core called rachis. When nuclei reach the gonad flexure, some of them undergo programmed cell death, while the remaining nuclei exit from pachytene and enter diakinesis to begin oogenesis.

Numerous genes were identified that regulate the germ line nuclei development from the distal tip part of the gonad to the proximal center. LAG-2 Delta in the distal tip and GLP-1 Notch in germ line are required to maintain the mitotic stem cell fate in the distal tip cell niche and to repress meiotic differentiation of germ line nuclei. As germ line nuclei leave the niche, the meiotic differentiation factors GLD-1, 2, and 3 and NOS-1 promote meiosis and repress GLP-1 translation and the mitotic fate. At the end of the transition zone, meiotic nuclei reorganize to the cortex to form the rachis. Meiotic nuclei arrest in pachytene until they reach the gonad flexure where Ras/Map kinase signaling promotes the pachytene nuclei into diakinesis. Mutations of *glp-1* and *gld-1* result in misregulated germ line transition from mitosis to meiosis. In *glp-1* gain-of-function alleles and *gld-1* loss-of-function alleles, the pachytene stage nuclei re-enter mitosis and resume the ability to proliferate (Francis, R. et al. 1995 and Pepper, A.S. et al. 2003). The over-generated mitotic nuclei fill the gonad and result in a proximal germ line tumor phenotype.

C. elegans germ line morphology is very well maintained throughout the adulthood of hermaphrodite *C. elegans*. Interestingly, one *fli-1* mutation we found, *ky535*, disrupted this germ line organization and caused misplaced germ line nuclei to form chains and span the rachis. This novel germ line phenotype was highly penetrant, with 94% of the adult animals exhibiting this phenotype. Since this phenotype affect germ line morphogenesis, we named it the Glm phenotype. While much is known about meiotic specification, less is known about the molecular mechanisms that control the reorganization of nuclei to the germ line cortex to form the rachis in the meiotic zone. The novel phenotype observed in *fli-*

1(ky535) mutants provides us a great tool to study the molecular mechanisms behind the rachis organization. With the convenience and consistency of this Glm phenotype, we studied the interaction of *fli-1* with other essential genes, such as *let-60 Ras*, *FLAP* and *gld-1*. The experiments presented here suggest that *C. elegans* FLI-1 acts with LET-60 Ras and FLAP to control the coordination of germ line nuclei meiotic differentiation with the germ line rachis morphogenesis and *fli-1* mutation suppress the germ line tumor formed in *gld-1* mutant background.

CHAPTER II

The actin-binding protein FLI-1 flightless-1 acts with LET-60 Ras to control germ line morphogenesis in *C. elegans*

2. 1. Abstract

The *C. elegans* germ line is a syncytial organ with dynamic morphogenesis. At the distal tips of the syncytial gonad, germ cell nuclei are mitotic and have stem cell character. As the syncytial nuclei move proximally, they enter meiosis and become arranged regularly at the germ cell plasma membrane, forming a single layer of nuclei around the nucleus-free center (the rachis). Fingers of germ cell plasma membrane invaginate around the nuclei but do not completely enclose them. Here we report that mutations in a *fli-1* gene encoding an actin-binding protein FLI-1 disrupt normal rachis organization. In *fli-1(ky535)* mutants, rows of meiotic germ nuclei were often seen in the central rachis. We found that loss-of-function and dominant-negative mutations in the *C. elegans* K-Ras homolog LET-60 as and in other Ras pathway components also caused the germ cell phenotype. Constitutively-active LET-60 Ras partially rescued the germ cell defect in both *fli-1(ky535)* and *fli-1(tm362)*, suggesting that that FLI-1 and LET-60 Ras control a similar process in germ cell morphogenesis. LET-60 Ras has been shown to control multiple aspects of germ cell development, including meiotic entry and exit from pachytene to diakinesis. These data suggest that LET-60 Ras coordinates changes in morphology involving FLI-1 that accompany other events in germ cell development.

2. 2. Introduction

Morphogenesis is one of the most important fundamental questions of developmental biology. Distinctively shaped cells form different types of tissues and therefore form organs and entire organisms. Tumor cells usually display abnormal morphology than their wild-type counterparts, which suggest that the regulation of morphogenesis is one of the key processes that contribute to tumor formation. Studies of morphogenesis are crucial to understand normal organogenesis and cancer biology.

The *C. elegans* germ line displays morphology changes from the distal tip to the proximal center. Each *C. elegans* adult hermaphrodite contains a germ line with two gonad arms covered by somatic sheath cells. The distal part of germ line is a syncytium, whit multiple germ line nuclei sharing a common cytoplasm. The germ line nuclei are generated by germ line stem cells located at the distal tip part of each gonad arm. Distal tip cells (DTC), providing the stem cell niche, cover the very distal part of the gonad and extend projections into the interior region of the gonad to contact with the germ line stem cells and regulate germ line stem cell proliferation. When germ line stem cells proliferate, they renew themselves as well as generate differentiated germ line nuclei. Differentiated germ line nuclei migrate from the distal gonad to the proximal central of the gonad after they are born. As the nuclei proceed proximally down the germ line, they lose the mitotic character and enter meiosis (the transition zone). Accompanying entry into meiosis is a reorganization of the nuclei in the germ cell syncytium. Mitotic germ nuclei at the distal tip are present throughout the germ cell volume. As the nuclei

enter meiosis, they associate with the germ cell cortex resulting in a nucleus-free inner core of cytoplasm called the rachis. This region of the distal gonad containing nuclei at the cortex and an inner rachis is called the meiotic pachytene zone. Thus, meiotic differentiation is coordinated with a morphogenetic event (the rearrangement of germ nuclei to the cortex). As nuclei reach the flexure of the gonad arm, individual meiotic nuclei undergo oogenesis and become completely enclosed by plasma membrane. Oocytes are fertilized as they move proximally through the spermatheca. This process of germ line organogenesis is dynamic and occurs throughout the fertile life of an adult hermaphrodite, but not much is known about how the rachis formation is regulated.

Described here are studies of a molecule, FLI-1 Flightless-1, that controls rachis formation without apparently affecting mitotic or meiotic specification. In *fli-1* mutants, chains of germ nuclei were observed in the rachis of the meiotic zone, and ultrastructural analysis revealed these nuclei remained associated with germ cell plasma membrane as well as sheath cell projections (a germ line morphogenesis defect, here called the Glm phenotype). No defects in mitotic or meiotic specification were observed in the misplaced nuclei or in any germ nuclei in *fli-1* mutants, and *fli-1* mutants displaying the Glm phenotype were viable and fertile.

fli-1 encodes a molecule with 17 N-terminal leucine-rich repeats (LRRs) and 5 C-terminal gelsolin repeats, similar to the *Drosophila* and human Flightless-1 molecules. *C. elegans* FLI-1 can bind to and sever actin filaments, and human Flightless-1, along with a monomer of G-actin, is a component of a transcriptional coactivator complex that acts with nuclear hormone receptors. In *Drosophila*,

Flightless-1 mutants display defects in flight muscle development (the root of the name *Flightless-1*) as well as defects in nuclear organization and cellularization in the syncytial blastoderm.

LRRs are often found in molecules that interact with Ras, and the *C. elegans* FLI-1 interacts with human Ha-Ras via the LRRs. Data presented here show that *let-60 Ras* mutants also display a *fli-1*-like Glm phenotype, and that *let-60 Ras* and *fli-1* interact genetically in the control of germ line morphogenesis. Thus, FLI-1 and LET-60 Ras might represent a novel pathway in the control of germ nucleus reorganization and rachis formation during meiotic differentiation in the *C. elegans* germ line.

2. 3. Materials and Methods

***C. elegans* strains and genetics.** *C. elegans* were cultured as described. All experiments were done at 20°C unless otherwise noted. The Bristol strain N2 was used as the wild-type. The following mutations and transgenes were used. LGX: *unc-115(mn481), sem-5(n2089)*. LGI: *mek-2(n1989), sur-2(ku9)*. LGII: *let-23(n1045), let-23(sy10), lin-31(n301)*. LGIII: *fli-1(ky535)*, *fli-1(tm362)*, *tnIs6[plim-7::gfp]*, *dpy-17(e164), unc-32(e189), mpk-1(ku1), eT1*. LGIV: *let-60(n2021)*, *let-60(s1124)*, *let-60(s1155)*, *let-60(s59)*, *let-60(sy93)*, *let-60(sy92)*, *let-60(sy99)*, *let-60(n1046)*, *let-60(n1700)*, *lin-3(e1417)*, *lin-3(n1058), lin-1(n431)*. LGV: *sos-1(s1031), lin-25(e1446), qIs56[lag-2::gfp]*.

Transgenic *C. elegans* were produced by germ line microinjection of DNA solutions using standard techniques. Cosmid DNAs were injected at 100ng/ml, and *fli-1* fragments generated by PCR were injected at 25ng/ml. To visualize germ line expression of *fli-1* transgenes, complex arrays were constructed using fragmented *C. elegans* genomic DNA in the injection mix. *fli-1::gfp* expression in the germ line was unstable and became non-visible as the transgenes were propagated. For the *fli-1::gfp* immunofluorescence experiments, new complex-array transgenic lines were produced before each experiment to ensure robust *fli-1::gfp* expression in the germ line.

The germ cell morphogenesis phenotype (Glm) was quantitated by scoring the percentage of gonad arms that displayed chains of nuclei spanning the rachis of the meiotic pachytene zone. In wild-type, chains of nuclei were often observed in the transition zone where reorganization occurs. Care was taken to

ensure that the Glm phenotype was scored clearly in the meiotic pachytene zone and not in the transition zone. Significance of quantitative data was determined by the t-test and by Fisher's Exact analysis (for percentages).

***fli-1* molecular biology.** Fragments of the *fli-1* gene were amplified using polymerase chain reaction (PCR). The sequences of all coding regions generated by PCR were determined to ensure that no errors were introduced. The *fli-1* whole gene consisted of bases 8,684,714 - 8,674,953 of linkage group III. For *fli-1(ky535)* sequencing, this region was amplified in three overlapping fragments and their sequences determined. In three separate amplifications, no nucleotide changes were detected in *fli-1(ky535)* DNA. The full-length *fli-1::gfp* transgene was produced by amplifying a region including the *fli-1* upstream and *fli-1* coding region but not including the stop codon or downstream region (bases 8,684,714-8,676,004 linkage group III). This fragment was then fused in-frame to *gfp* in vector pPD95.77. The *fli-1 promoter::gfp* fusion was produced by amplifying the *fli-1* upstream region (8,684,714 to 8,683,600 of linkage group III) and fusing the fragment upstream of *gfp* in pPD95.77. RNA-mediated gene interference (RNAi) was performed by microinjection of double-stranded RNA, representing a portion of *fli-1* exon 6 (see Figure 4), into the germ line and analyzing the germ cell phenotype in progeny of injected animals. The sequences of all oligonucleotide primers used in this study are available upon request.

Transgene expression. To reduce the transgene silencing phenomenon in *C. elegans* germ line, when the rescuing *fli-1::gfp*, *fli-1* containing cosmid B0523, *fli-1* PCR products and *fli-1 promoter::gfp* were expressed in animals, each of these was introduced into *C. elegans* germ line by co-injecting with digested wild-

type *C. elegans* genomic DNA.

Imaging and microscopy. Differential Interference Contrast (DIC) and epifluorescence images were taken using a Leica DMR compound light microscope with a Hamamatsu Orca digital camera. TEM images were collected using a Jeol transmission electron microscope with digital camera. Confocal images were obtained on Zeiss Meta spectral imaging upright confocal microscope. Images were processed in Adobe Photoshop.

TEM specimen preparation. 12-hour-old adult hermaphrodite animals were fixed by a modified two-step fixation based upon previous techniques (David H. Hall, 1995). Animals were anaesthetized using 8% EtOH in M9 buffer for 5 minutes. Animals were then placed in glass well slides and marinated with fixation solution (2.5% glutaraldehyde, 1% formaldehyde in 0.1M sucrose, 0.05M cacodylate, pH7.4) on ice for 30 minutes. Animals were then cut in half using a scalpel and incubated in fixation solution overnight at 4°C. Animals were then rinsed on ice 3 times with 0.2M cacodylate for 10 minutes each, incubated with 0.5% OsO_4, 0.5% $KFe(CN)_6$ in 0.1M cacodylate for 90 minutes on ice followed by three 10-minute 0.1M cacodylate buffer washes. Specimens were stained in 1% uranyl acetate in 0.1M sodium acetate, pH 5.2, for 1 hour at room temperature, followed by three 5-minute 0.1M sodium acetate washes and three 5-minute distilled water washes. Worms were packed in parallel in a V-shaped plexiglass trough and were embedded 3% seaplaque agarose. Approximately 1mm2 blocks then were dehydrated in acetone and embedded in Embed 812 (Dentler and Adams 1992)

Cross-sections of worms were cut using a diamond knife and Leica

microtome and were picked up on carbon-over-formvar coated single hole grids. Sections were dried overnight and then stained using minor modifications of the Hall (1995) procedure. Stains and washes were prepared in 16 well plastic culture dishes at room temperature. Grids were stained in 1% uranyl acetate, 50% methanol for 15 minutes, rinsed twice (30 seconds each) with 100% ethanol followed by 50% ethanol/water (15 seconds), 30% ethanol/water (15 seconds), and four 15 second washes in water. Sections then were stained for 5 minutes with 0.1% lead citrate in 0.1M NaOH, rinsed twice with 0.02M NaOH (1 minute/change), rinsed five times in water (15 seconds/wash) and were air-dried before examination with the TEM.

DAPI staining of dissected gonads. The gonads of 12-hour-old adult hermaphrodite animals were dissected and fixed with 3% paraformaldehyde containing 0.1M K_2HPO_4, pH7.2, for 1 hour at room temperature. The specimens were washed once with phosphate-buffered saline (PBS) with 0.1% Tween-20 (PBT) for 5 minutes followed by treatment with 100% methanol for 5 minute at -20°C. Specimens were treated with PBS containing 100ng/ml 4',6-diamidino-2-phenylindole (DAPI) for 10 minutes at room temperature followed by three washes in PBT. Gonads were mounted on a 2% agarose pad in M9 buffer with 1mg/ml 1,4-diazabicyclo[2.2.2]octane (DABCO) antifade reagent.

BrdU labeling of dissected gonads. *Escherichia coli* strain MG1693 (a thymidine-deficient *E. coli* strain kindly provided by the *E. coli* stock center) were grown minimal medium (M9) with 0.4% glucose, 1mM $MgSO_4$, 1.25 μg/ml vitamin B1, 0.5 μM thymidine, and 10 μM bromodeoxyuridine (BrdU) overnight

at 37°C (Crittenden S. L., *et al.,* 2006). BrDU-labeled *E. coli* were then plated on nematode growth medium (NGM) plates containing 100μg/ml ampicillin. 12-hour-old adult hermaphrodite animals were placed on seeded plates and allowed to eat the BrDU-labeled *E. coli* for varying times depending on the experiment (usually 5 minutes). Gonads were dissected immediately and fixed in methanol at -20°C for 1 hour followed by 1% paraformaldehyde for 15 minutes at room temperature.

Fixed gonads were placed in 1mg/ml BSA in PBT for 15 minutes, 2N HCl to denature DNA for 30 minutes at room temperature, and 0.1M sodium borate to neutralize for 15 minutes at room temperature. The specimens were blocked in 1mg/ml BSA in PBT for 15 minutes and stained with a 1:2.5 dilution in PBT of anti-BrdU antibody (B44, Becton-Dickinson, San Jose, CA) at 4°C overnight. On the next day, the specimens were washed three times by 1mg/ml BSA in PBT for 10 minutes each. A 1:500 dilution of Alexa 488-conjugated goat-anti-mouse antibody was incubated with the specimens at room temperature for 2 hours in PBT. The specimens were washed three times with 1mg/ml BSA in PBT for 10 minutes each with DAPI in the last wash to stain DNA (see above). Gonads were mounted for microscopy as described above.

Anti-GFP immunofluorescence of dissected gonads. Gonads of 12-hour-old adult hermaphrodite animals were fixed as described for DAPI staining. Fixed gonads were blocked for 1 hour in 1mg/ml BSA in PBT at room temperature and then were incubated overnight with 1:50 diluted monoclonal anti-GFP antibody at 4°C. The specimens were washed three times with PBT for 10

minutes each and incubated with 1:500 diluted Alexa 488-conjugated goat-anti-mouse antibody for 2 hours at room temperature. DAPI was included to stain DNA. Stained gonads were rinsed three times with PBT for 10 minutes each. Gonads were mounted for microscopy as described above

2. 4. Results

The wild-type *C. elegans* germ line is a syncytial organ with dynamic morphogenesis. At the distal tips of the syncytial gonad, germ line nuclei are mitotic and have stem cell character (mitotic zone; Figure 2.1A). Distal tip cell (DTC; Figure 2.1A) covers the distal tip part of each gonad arm and provides a stem cell niche regulating the proliferation of germ line mitotic nuclei. In order to send regulatory signal to germ line mitotic nuclei, DTC produces filopodia extending into the distal tip part of gonad arm to contact with germ line mitotic nuclei. While germ line mitotic nuclei renew themselves during their proliferation, they also generate differentiated daughter nuclei that will travel from the distal tip to the proximal center of gonad. As the syncytial nuclei move proximally, they enter meiosis and remain in the pachytene stage of meiosis I (transition zone and pachytene; Figure 2.1A) and become arranged regularly at the germ line plasma membrane, forming a single layer of nuclei around the nucleus-free center (the rachis; Figure 2.1A). When the pachytene nuclei reach the reflex of the gonad, a number of nuclei undergo programmed cell death leaving only a fraction of the nuclei exit the pachytene stage and enter diakinesis to complete the oogenesis.

To ensure that the germine development occurs correctly, when germ line nuclei enter meiosis starting a meiotic differentiation, this event must coordinate with a germ line morphology change, forming a nucleus-free rachis. Thus, the *C. elegans* germ line provides us an excellent system to investigate the coordination of cell fate determination and cellular morphogenesis. Next in my thesis, I am going to discuss about the work I have done on studying *ky535* mutation that

disrupts the coordination of germ line meiotic differentiation and rachis organization.

***ky535* mutation is synthetic lethal with *unc-115(mn481)*.** The *ky535* mutation that I am discussing here was originally isolated as a synthetic lethal mutation with *unc-115(mn481)*. In *C. elegans, unc-115* gene encodes an actin-binding LIM Zn-finger protein involved in axon guidance and that is required for RAS signaling. *unc-115* is widely expressed in many tissues including all neurons, excretory-canal, pharynx and hypodermis. Surprisingly, *unc-115* mutants only exhibit moderate axon pathfinding defects and few defects in other tissues, indicating that other genes may act redundantly with *unc-115* in those tissues. An *unc-115(mn481)* synthetic lethal screen was performed by Dr. Erik A. Lundquist to identify genes that act redundantly with *unc-115*. *ky535* was one of those mutations identified by this screen.

unc-115(mn481);ky535 homozygous mutants have severe pharyngeal pumping defects, and those defects seriously affect the eating behavior which requires pharyngeal pumping (Figure 2.2). As a result, the *unc-115(mn481);ky535* homozygous mutants starve soon after hatching and arrest at L1 larval stage. The synthetic lethal phenotype of *unc-115(mn481);ky535* homozygous mutants suggests *unc-115* and *ky535* might have overlapping function in regulating pharyngeal pumping.

***ky535* mutants have germ line morphogenesis defects (here called Glm phenotype).** Although *unc-115(mn481);ky535* homozygous mutants were lethal, the *ky535* single mutants were viable and fertile and displayed a slightly dumpy body morphology. Although *unc-115* mutants had moderate defects in axon

pathfinding, *ky535* mutants did not have obvious defects in PDE, ventral cord and CAN neurons (defects in other types of neurons need further examination). *ky535* adult mutants exhibited defects in germ line morphogenesis that was observed by using differential interference contrast (DIC) microscopy (Figure 2.3B).

In *ky535* homozygous mutants, 94% of the gonad arms were defective comparing with wild-type animals (Figure 2.3A). In the germ line pachytene zones of *ky535* mutants, a majority of germ line nuclei were associated with the germ line plasma membrane but chains of apparently connected nuclei were observed spanning the rachis. Those chains of nuclei also moved proximally as normal germ line nuclei do (approximately one nucleus width/h, or 3-7μm/h) while they remained intact. Such chains of germ line nuclei were rarely if ever observed in wild-type gonad meiotic zone. This phenotype is called germ line morphogenesis phenotype (Glm) in the rest of my thesis.

***ky535* mutants have normal germ line meiotic development.** The Glm phenotype observed in *ky535* mutants could be explained by meiotic germ line nuclei re-entering mitosis in the pachytene zones. To test this hypothesis, a BrdU incorporation assay was performed. BrdU is a molecule that can be incorporated into DNA during the S phase of mitosis. As a consequence, when BrdU is present, the DNA of nuclei that are undergoing mitosis S phase will be labeled by BrdU, and the BrdU signal can be detected by anti-BrdU antibody. Wild-type animals and *ky535* mutants were fed with BrdU-labeled food for 10 minutes, and the gonads were dissected and stained with anti-BrdU antibody. After exposing to BrdU-labeled food for 10 minutes, for wild-type animals, BrdU was only incorporated into the mitotic nuclei located at the distal tip mitotic zones (Figure

2.3G). For *ky535* mutants, a similar BrdU labeling pattern was detected (Figure 2.3H). The misplaced nuclei in the rachis of *ky535* mutants did not incorporate BrdU, suggesting those nuclei did not synthesize DNA and still remained in meiosis instead of re-entering mitosis. The exposure time to BrdU-labeled food was increased to 2 hours and still no apparent differences between wild-type and *ky535* mutants were detected. Therefore, Glm phenotype in *ky535* mutants is not due to meiotic nuclei re-entering mitosis, indicating that those misplaced nuclei are still in meiosis. DAPI staining was also carried out to assay the nuclear morphology in *ky535* mutated germ line. As a result from DAPI staining, nuclei in *ky535* mutated germ line progressed normally from a mitotic morphology (chromosomes condensed around a chromosome-free core and the occasional nucleus in mitotic metaphase or telophase); through a transition zone of mixed mitotic and meiotic morphologies; to a meiotic pachytene morphology (distinctive "bowl of spaghetti" morphology resulted from side-by-side aligned homologous chromosomes). When focusing on DAPI stained misplaced germ line nuclei in *ky535* mutants, they displayed pachytene morphology ("bowl of spaghetti"; Figure 2.3I), supporting the BrdU incorporating results. Transmission electron microscopy (TEM) was also used to investigate the ultra structure of *ky535* mutants. Under TEM, mitotic nuclear envelope displayed an irregular shape (Figure 2.4D), while meiotic nuclear showed a more smooth and round shaped nuclear envelope (Figure 2.4A). Misplaced nuclei in pachytene zones of *ky535* mutants displayed a round, regular appearance envelope same as normal meiotic nuclei under TEM (Figure 2.4B and C). All of the evidence indicates that the germ line nuclei development from mitosis to meiosis is remained normal in

ky535 mutants. Thus this Glm phenotype in *ky535* mutants is due to disruption of rachis organization but not meiotic nuclei re-entering mitosis.

Chains of misplaced germ line nuclei span the rachis and remain associated with sheath cells in *ky535* mutants. The distal half of the bi-lobed *C. elegans* gonad is a syncytium, with multiple germ line nuclei sharing a common cytoplasm. In the meiotic zones of wild-type gonad, meiotic nuclei are associated with the cortex, and incompletely covered by germ cell plasma membrane. The germ cell plasma membrane protrudes between each nucleus and forms the characteristic "T" structures of membrane between each nucleus (Figure 2.5A and Figure 2.4A). The gonad is then partially wrapped by multiple somatic gonadal sheath cells, which extend filopodia fill the gaps between nuclei formed by "T" structure. Those sheath cell protrusions do not extend deeply into the rachis. The basement membrane further envelops the entire gonad. In *ky535* mutants, chains of misplaced meiotic nuclei were observed in the rachis of meiotic zones. For those misplaced germ line nuclei, they might remain associated with membrane structure (sheath cells and/or germ cell plasma membrane) or become detached from the germ cell plasma membrane. To understand the *ky535* germ line defect at the ultrastructural level, cross-sections of *ky535* mutant gonads were analyzed by TEM and compared with TEM cross-sections from wild-type gonads. In wild-type gonad meiotic zone TEM cross-sections, "T" structures were obviously observed near the cortical nuclei (Figure 2.4A). In the cross-sections of *ky535* mutant gonad meiotic zones, "T" structures were also clearly visualized near cortical nuclei. Even for misplaced nuclei, germ cell plasma membrane was still associated with them, and mostly resembled the "T" structures that normally form near cortical

nuclei (Figure 2.4B and C and Figure 2.6A and B).

In between germ cell plasma membrane that associated with misplaced germ line nuclei in *ky535* meiotic zone TEM cross-sections, additional membrane structures were detected (Figure 2.6B and C). As described earlier, in wild-type gonad, somatic sheath cells partially wrap the germ cell and fill the gaps between each nucleus by extending filopodia, raising the possibility that the additional membrane structures detected in *ky535* are extensions of somatic sheath cells. To address this possibility, a *lim-7::gfp* reporter gene was used to drive GFP expression in the cytoplasm of the somatic sheath cells. In wild-type animals expressing *lim-7::gfp*, no GFP fluorescence was observed in the rachis of germ line meiotic zones (Figure 2.7A and D), although GFP expression was detected on the surface of the gonad in a honeycomb pattern resulting from filling the gaps between each nucleus by sheath cells (Figure 2.8A). However, in *ky535* mutants expressing *lim-7::gfp*, patches of GFP expression were observed in the rachis of germ line meiotic zones. This additional sheath cell expression in the rachis was always associated with misplaced germ line nuclei, suggesting the misplaced germ line nuclei were still associated with sheath cells (Figure 2.7B and E). A *lag-2::gfp* transgene, expressed only in the distal tip cell, did not show these patches in the rachis of *ky535* mutants (Figure 2.9C and D), indicating that only the more proximal sheath cells were associated with the misplaced germ line nuclei. Furthermore, the *lim-7::gfp* cortical honeycomb expression pattern in *ky535* mutants was disorganized, indicating cortical nuclei were disorganized (Figure 2.8B). The *lim-7::gfp* expression data together with the TEM results indicate that sheath cell protrusions extended into the interior gaps between misplaced germ

cell plasma membrane and nuclei in the rachis of *ky535* mutant gonads as diagrammed in Figure 2.5B.

***ky535* mutant rachis organization resembles wild-type mitotic zone organization.** In wild-type gonads, at the ultrastructural level (TEM cross-sections), the distal tip cell covered the distal tip part of gonad and extended filopodia into the interior gaps between mitotic germ line nuclei (Figure 2.6D). The mitotic nuclei with irregular-shaped envelope were arranged next to each other without forming a rachis in the mitotic zone (Figure 2.4D). At the beginning of transition zone, the germ line nuclei entered meiosis and became round-shaped (Figure 2.4E). At this point, rachis has not formed completely yet. As they move further into the meiotic zone, meiotic nuclei covered by round-shaped envelop became associated with the cortex and were partially covered by germ cell plasma membrane, forming a nucleus-free rachis. Thus, coordinating with germ line nuclei meiotic differentiation (entering the meiotic zone), the germ line was undergoing a morphology change, forming the rachis.

For *ky535* mutant gonads, at the ultrastructural level, even in the meiotic zone, rachis was not formed correctly, with meiotic-appearing nuclei covered by germ cell plasma membrane spanning the rachis. Occasionally, sheath cell protrusions were visualized in between misplaced nuclei. This meiotic zone organization in *ky535* mutant gonads was similar to structures observed in the mitotic zone of wild-type gonads, which had protrusions extending out from distal tip cell in between of mitotic nuclei and did not have a rachis formed. Thus the coordination of germ line nuclei meiotic differentiation and rachis organization was disrupted in *ky535* mutant gonads.

***ky535* mutant gonads are misshapen and contain more nuclei than wild-type.** As judged by TEM cross-sections, the diameter of the gonad in wild-type animals was consistent throughout the meiotic zone (approximately 20μM). Gonad diameter was irregular in *ky535* mutants, including regions of larger diameter (compare Figure 2.4A, B and C) and regions where the gonad was apparently constricted.

The meiotic nuclei in *ky535* were of roughly the same size and shape as those in wild-type (Figure 2.4 and Figure 2.10). However, *ky535* had on average more nuclei per section than wild-type (Figure 2.4 and Figure 2.10). The excess nuclei could be explained by the misplaced nuclei in the rachis, as counts of nuclei at the cortex of the germ line were nearly equivalent in *ky535* mutants and wild-type (Figure 2.10). *ky535* on average had more germ line nuclei per TEM cross-section than wild-type. The germ line nuclei in each gonad arm were counted by staining germ line with DAPI. Each wild-type gonad arm on average had 653.75±21.69 germ line nuclei (n=4), while each *ky535* gonad arm on average had 693.63±40.20 germ line nuclei (n=8). The P-value for this test was 0.0478. This slight number difference of germ line nuclei was consistent with the results from TEM cross-sections. Although *ky535* mutant gonads produced more germ line nuclei than wild-type gonads, *ky535* mutants gave rise to approximately the same number of progeny compared with wild-type animals. As discussed earlier when pachytene nuclei reach the flexure of the gonad and oogenesis begins, a fraction of nuclei undergo apoptosis and only a number of germ line nuclei can complete oogenesis. *ky535* mutants displayed a greater number of germ line nuclei undergoing apoptosis at the gonad flexure than did wild-type, as assayed by

GFP-tagged CED-1 in the somatic cells of the gonad, a marker for engulfment of apoptotic germ line nuclei (Figure 2.10). Thus, although *ky535* mutant gonads contained more germ line nuclei than wild-type gonads, it is possible that the excess germ line nuclei were prevented from undergoing oogenesis by additional apoptosis.

***ky535* is an allele of the *fli-1* gene.** Using the synthetic lethal phenotype of *unc-115(mn481); ky535* double mutants, *ky535* mutation was mapped genetically to the linkage group III by standard linkage analysis with visible markers [*unc-115(mn481); dpy-5* for linkage group I, *unc-115(mn481); dpy-10* for linkage group II, *unc-115(mn481); dpy-17* for linkage group III, *unc-115(mn481); dpy-13* for linkage group IV, *unc-115(mn481); dpy-11* for linkage group V] *ky535* is not on the X chromosome, since when *unc-115(mn481)* males were crossed with *unc-115(mn481); ky535; KyEx209* [*KyEx209* was a GFP-tagged wild-type copy of *unc-115*. So, when GFP-tagged *KyEx209* was expressed, it rescued the *unc-115(mn481)*, as a consequence the *unc-115(mn481); ky535; KyEx209* were viable], the resulting non-GFP expression males [*unc-115(mn481); ky535*] were not lethal. Using the Glm phenotype, *ky535* mutants were crossed with marker strain *dpy-17 unc-32* on linkage group III to do the three-factor mapping. *ky535* was mapped close to and to the left of *unc-32* (approximately 0.22 cM) (Figure 2.12A). The *fli-1* gene (B0523.5), which encodes an actin-binding protein of the Flightless-1 family, resides in this region of the genome (Figure 2.12B and C). *ky535* was isolated through synthetic lethal screen with a mutation in *unc-115*, which encodes an antin-binding protein, raising the possibility that *ky535* also affects a gene that encodes an actin-binding protein. *fli-1* is the only gene that

encodes an actin-binding protein in this region. The possibility that *ky535* affected *fli-1* was explored. RNA interference (RNAi) of *fli-1* was performed. *fli-1*(RNAi) animals produced the same Glm phenotype as *ky535* mutants (Figure 2.3F and Figure 2.13). Furthermore, the cosmid B0523, which contains *fli-1*, rescued the synthetic lethality of *unc-115(mn481); fli-1(ky535)* animals (Figure 2.12B). The B0523 cosmid also contains two other genes, B0523.1 and B0523.3. RNAi of these genes did not phenocopy the germ line defects of *ky535*. Additionally, a fragment of B0523 containing only the *fli-1* gene and a tryptophan tRNA (Figure 12C) rescued the synthetic lethality of *unc-115(mn481); fli-1(ky535)* mutants (Figure 12C), and a *fli-1:: gfp* full-length fusion transgene partially rescued the germ line defects of *fli-1(ky535)* animals (Figure 2.13) as well as the lethality of *unc-115(mn481); fli-1(ky535)* double mutants. These results indicated that *ky535* affects the *fli-1* gene. The nucleotide sequence of the entire region included in the rescuing *fi-1(+)* transgene was sequenced from *ky535* mutants. No nucleotide changes were detected in two independent PCR amplifications of the *fli-1* gene from *ky535* genomic DNA. Possibly, *ky535* is regulatory mutation outside of the region necessary for rescue, and transgenic *fli-1(+)* expression, which can often lead to overexpression, can overcome the *ky535* mutation.

The Glm phenotype observed in *fli-1(ky535)* mutant might be autonomous to the germ line. In *ky535* mutant gonads, chains of misplaced meiotic nuclei spanned the rachis while remaining associated with sheath cell protrusions. Possibly, the defects are in the somatic sheath cells, which extend longer than normal and drag the attached nuclei cross the rachis. To address this possibility, adult male *ky535* mutant animals were checked under DIC, since male

gonads do not contain somatic sheath cells. Even when somatic sheath cells are not present in males, chains of misplaced germ line nuclei were observed in the gonads of *ky535* mutant males (Figure 2.11A and B), indicating the Glm phenotype seen in *ky535* mutants are due to defects in germ line but not the somatic sheath cells. To further confirm that the Glm phenotype is due to defects in germ line, the *fli-1* RNAi was performed in *rrf-1(ok589)* and *rrf-1(pk1417)* mutants. *rrf-1* mutants are sensitive to RNAi in germ line, but RNAi interference for genes expressed in somatic tissue, such as somatic sheath cells, is lost in *rrf-1* mutants. Therefore, if *fli-1* RNAi makes *rrf-1* mutants display Glm phenotype, it will provide better evidence to support that the Glm phenotype is due to germ line defects but not the sheath cell defects. Consistent with this hypothesis, the *fli-1* RNAi made both *rrf-1* alleles, *ok589* and *pk1417* produce the same Glm phenotype as seen in *fli-1(ky535)* mutants (Figure 2.11C and D). Furthermore, as shown below, *fli-1* is expressed in germ line but not somatic sheath cells (Figure 2.14A). All of these data strongly suggest that the Glm phenotype observed in *fli-1(ky535)* might be autonomous to the germ line.

A deletion allele of *fli-1*, *tm362*, causes the same Glm phenotype. To confirm that disruption of the *fli-1* gene resulted in the Glm phenotype, a deletion allele of the *fli-1* gene was analyzed (isolated and kindly provided by the The National Bioresource Project for the Experimental Animal *C. elegans*, S. Mitani). The *tm362* deletion removed bases 10973 to 11931 relative to the cosmid B0523 (Genbank Accession number L07143) with breakpoints in coding exons 9 and 11 of *fli-1* (Figure 2.12C). The *tm362* deletion removed coding region for tyrosine 820 to methionine 1070 in the FLI-1 polypeptide, encompassing parts of gelsolin

domains 3 and 4 (Figure 2.12D). A fusion of the *tm362* breakpoints would result in a frameshift and the introduction of a premature stop codon 105 nucleotides (35 amino acid residues) after the breakpoint.

fli-1(tm362) homozygotes were lethal, and the homozygous embryos arrested during embryogenesis and failed to hatch (details will be discussed in Chapter III). Although the *fli-1(tm362)* homozygotes were lethal, the heterozygous *tm362/+* animals were viable and displayed Glm phenotype as same as *fli-1(ky535)* mutants (Figure 2.3E and Figure 2.13), suggesting that the *fli-1* locus is haploinsufficient for the germ line morphogenesis phenotype. Homozygous *fli-1(tm362)* animals were lethal, but homozygous *fli-1(ky535)* were viable and heterozygous *ky535/+* animals also displayed Glm phenotype (60% compared to 94% for *ky535* homozygotes; Figure 2.13), indicating that *ky535* is a hypomorph allele of *fli-1.* Trans-heterozygous *ky535/tm362* animals were viable and had a severe germ cell defect (91%; Figure 2.13), suggesting that *ky535* and *tm362* failed to complement each other for the Glm phenotype. However, the additive effect of each heterozygote alone could explain this effect, so the possibility of complementation cannot be excluded.

The *fli-1::gfp* full-length fusion transgene rescued the lethality of *fli-1(tm362)* mutants, and the rescued *fli-1(tm362)* animals displayed a significantly less severe Glm phenotype than *fli-1(ky535)* homozygotes (Figure 2.13). Together, these data suggest that *ky535* is a hypomorphic, incomplete loss of function *fli-1* allele; that a stronger *fli-1* allele, *tm362,* leads to embryonic arrest; and that the *fli-1* locus is haploinsufficient for the Glm phenotype (i.e. reduction of *fli-1* gene dose by half results in a germ line morphogenesis phenotype).

***fli-1* is expressed in the germ line and in muscle.** *fli-1* mutants, *ky535* and *tm362/+*, displayed Glm phenotype, suggesting *fli-1* has function in regulating germ line morphogenesis. Therefore, *fli-1* gene should be expressed in germ line. To analyze the *fli-1* expression pattern, the *fli-1* promoter (*fli-1* 5' upstream region) was fused with GFP to detect the *fli-1* promoter expression pattern. p*fli-1::gfp* expression was observed in the germ line of hermaphrodites and males and displayed a honeycomb pattern due to the exclusion of GFP from the germ line nuclei (Figure 2.14A). The p*fli-1::gfp* honeycomb expression pattern detected in germ line was not due to expression in the sheath cells, since the similar expression pattern was also observed in male gonads, which have no sheath cells (Figure 2.14A inset). Additionally, p*fli-1::gfp* expression was observed throughout the entire germ line whereas the sheath cell *gfp* expression does not cover the entire germ line. p*fli-1::gfp* was also expressed in the pharyngeal muscle [consistent with the feeding defects of *fli-1(ky535)*], vulval muscle and body wall muscle (described in Chapter III) (Figure 2.14B).

The full-length *fli-1::gfp* associates with germ line nuclei. The full-length *fli-1::gfp* transgene, predicted to encode a full-length FLI-1 polypeptide with GFP at the C-terminus, rescued *fli-1* lethality and rescued the germ line defects of *fli-1(ky535)* and *fli-1(tm362)* (Figures 2.13). The full-length *fli-1::gfp* expression was driven in the germ line from complex extrachromosomal arrays (see Materials and Methods). Gonads from animals expressing *fli-1::gfp* were dissected and stained with anti-GFP antibody. Specific GFP immunoreactivity was predominantly associated with germ line nuclei (Figure 2.15A-F). Gonads from animals without the *fli-1::gfp* transgene showed no such reactivity (Figure 2.15G-

I). *fli-1::gfp* expression often appeared punctate, and did not overlap exclusively with chromatin as judged by DAPI co-staining (Figure 2.15D-F). No difference in *fli-1::gfp* expression accumulation or nuclear association was detected along the length of the distal gonad from the mitotic zone through the meiotic zone.

***F57B9.7* encodes a double stranded RNA binding protein, which might assist FLI-1 function in nucleus.** Full-length *fli-1::gfp* was associated with germ line nuclei, suggesting FLI-1 might have function in the nucleus. Several potential NLSs (Nuclear Localization Signals) were found within the FLI-1 region by using PSORT II Server, such as pat4: RRRK at 435-438 aa, pat4: KPRK at 1226-1229 aa, pat7: PNDARKK at 381-387 aa. In addition, other proteins may also assist FLI-1 translocation by forming a complex.

The protein encoded by *F57B9.7* is called FLAP (FLI1 LRR associated protein) that binds to LRRs of FLI-1. FLAP protein region also contains several potential NLSs, such as pat4: RRRP at 9-12 aa, pat7: PSSGRRR at 5-11 aa. To address the possibility that FLAP can be expressed in the nucleus, the full-length *flap::gfp* expression construct was generated. The *flap::gfp* expression was detected in the pharynx and body wall muscle, and was localized to the nucleus (Figure 2.19). To further investigate the role of FLAP, RNA interference (RNAi) of *flap* was performed. As predicted, *flap* (RNAi) animals produced the same Glm phenotype as *fli-1 (ky535)* mutants (Figure 2.20). These data indicate that FLAP may interact with FLI-1 through the N-terminus LRRs of FLI-1 and control germ line morphology together. Since FLAP expression was detected in the nucleus, FLAP may assist to translocate FLI-1 into the nucleus.

LET-60 Ras is involved in controlling germ line morphogenesis. *fli-1*

encodes a LRRs containing actin-binding protein. It has been shown that LRRs of *C. elegans* FLI-1 can physically interact with human Ha-Ras. LET-60 Ras in *C. elegans* controls several aspects of germ line development, such as the transition from meiotic pachytene to diakinesis. Possibly, this LET-60 Ras in *C. elegans* germ line can interact with *fli-1* in regulating the germ line morphogenesis. To address that possibility, multiple alleles of *let-60* Ras were scored for the Glm phenotype in germ line by DIC. All of the loss-of-function alleles and dominant negative alleles of *let-60* Ras displayed the same Glm phenotype as *fli-1(ky535)* mutants, but not the constitutively active *let-60* Ras alleles (Figure 2.16A). The loss-of-function *let-60* allele *n2021* caused a *fli-1(ky535)*-like Glm phenotype in 44% of gonad arms, and the stronger *let-60* loss-of-function alleles *s1124, s1155,* and *s59*, which are homozygous lethal, caused the Glm phenotype in the gonad arms of heterozygous animals (52%, 23%, and 47%, respectively). Three different dominant-negative alleles of *let-60* also displayed the same Glm phenotye as homozygotes or as heterozygotes (e.g 94% for homozygous *sy93*) (Figure 2.16A). However, the constitutively active *let-60* alleles, *n1700* and *n1046* caused little or no Glm phenotype Figure 2.16A). These data suggest that *let-60* Ras is also involved in controlling the germ line morphogenesis as *fli-1.* Additionally, by expressing p*lim-7::gfp* in sheath cells, sheath cell protrusions were also detected in the rachis of loss-of-function and dominant negative alleles of *let-60* (Figure 2.6C and F), associating with misplaced chains of germ line nuclei. Furthermore, TEM cross-sections *let-60 (n2021)* showed the similar ultrastructural defects as *fli-1(ky535).* Combining these results, loss-of-function and dominant negative alleles of *let-60* cause the same Glm defects as *fli-1(ky535)*. Therefore, *let-60* Ras

in *C. elegans* also regulates germ line morphogenesis in a manner similar to *fli-1*.

LET-60 Ras signaling pathway is activated by the binding of epidermal growth factor (EGF LIN-3) to epidermal growth factor receptor (EGFR LET-23). The autophosphorylation of specific tyrosine residues in the cytoplasm domain of EGFR creates binding sites for SEM-5 (a SH domain 2 and 3-containing adaptor protein), which can further bind a with guanine nucleotide exchange factor (EGF SOS-1). SOS-1 activates LET-60 Ras. Activation of LET-60 Ras subsequently activates the LIN-45 Raf and mitogen-activated protein kinase pathway, which ends up activating multiple transcription factors, such as LIN-1 and LIN-25. The results discussed earlier shows that LET-60 Ras involved in regulating germ line morphogenesis. To investigate whether LET-60 Ras regulates germ line morphogenesis through the canonical LET-60 pathway, mutations in the genes encoding components of this pathway (*lin-3, let-23, sem-5, sos-1, lin-45, mpk-1, lin-1, sur-1, lin-25, lin-3*) were analyzed for the Glm phenotype. Mutations in *sem-5, sos-1, mpk-1, lin-1, sur-2* and *lin-25* all caused the Glm phenotype, indicating those components are involved in regulating germ line morphogenesis also. Interestingly, the mutations of genes encoding EGF and EGFR, *lin-3* and *let-23*, did not display Glm phenotype, which suggests a distinct ligand and receptor complex might activate the LET-60 pathway in regulating germ line morphogenesis.

LET-60 and FLI-1 act together to control germ line morphogenesis. Loss-of-function alleles and dominant negative alleles of *let-60* Ras displayed the same Glm phenotype as *fli-1(ky535)* mutants, suggesting that LET-60 Ras and FLI-1 may have the same function in regulating germ line morphogenesis. To

investigate whether they function together, constitutively-active *let-60* mutant alleles, *n1700* and *n1046*, were used to rescue *fli-1(ky535)* and *fli-1(tm362)/+* mutants. Constitutively-active *let-60* alleles, *n1700* and *n1046*, which presumably cause *let-60* overactivation, had no apparently effect on germ line morphogenesis (Figure 2.16A). But when made double with *fli-1* mutants, *let-60(n1700)* partially suppressed the Glm phenotype of *fli-1(ky535)* heterozygotes and homozygotes as well as *fli-1(tm362)/+* heterozygotes (Figure 2.16B). Another constitutively-active *let-60* allele, *n1046*, also partially suppressed the Glm phenotype of *fli-1(ky535)/+* heterozygotes. These results suggest that *let-60* Ras and *fli-1* genetically act together to control germ line morphogenesis.

2. 5. Discussion

Ras proteins are GTPases, and are well recognized for their essential function in transducing extracellular signals that regulate cell growth, survival, and differentiation. Cellular *ras* genes were identified as dominant oncogenes in various types of tumors and are involved in oncogenesis. *C. elegans* LET-60 Ras controls several aspects of germ line development including the exit of meiotic germ line nuclei from pachytene stage to diakinesis. Previous studies have shown that *C. elegans* FLI-1 N-terminus LRRs can physically interact with human Ha-Ras. The genetic analysis described here suggest that LET-60 Ras has a novel function in regulating germ line morphogenesis and FLI-1 is a novel factor in Ras signaling pathway. Our studies show that overactivity of *let-60* Ras can compensate for *fli-1* loss-of-function in germ line, suggesting that FLI-1 and LET-60 Ras act together to control germ line morphogenesis.

***flightless 1* controls syncytial morphogenesis in *Drosophila* and *C. elegans*.** *Drosophila* embryogenesis begins with the formation of zygote. Following fertilization, the zygote undergoes 13 rounds of mitosis (nuclear division) in the absence of cytokinesis, resulting a syncytial blastoderm. After the eighth nuclear division, most of the nuclei migrate to the cortex of the egg. The nuclei on the cortex keep dividing and eventually form a monolayer of 6000 nuclei or so. These nuclei are partitioned into separate cells by invagination of membranes from the surface of the egg between each nucleus. This process, termed cellularisation, makes the *Drosophila* embryo develop from syncytial blastoderm stage to cellular blastoderm stage (a monolayer of cells are regularly

aligned at the periphery of the egg) (Figure 2.17A).

For *flightless 1* mutant *Drosophila* embryos, until the beginning of cellularisation, they are indistinguishable from wild-type embryos. However, cellularisation is defective in *flightless 1* mutant *D rosophila* embryos. Incompletely cellularized nuclei are irregularly aligned at the cortex, with some nuclei losing their position and sinking towards the center of the egg. When gastrulation begins, nuclei in ventral cells move out of the incompletely cellularized peripheral layer of cytoplasm into the inside of the egg (Straub et al., 1996) (Figure 2.17B).

FLI-1 controls germ line organization in *C. elegans*. *fli-1* mutants displayed a novel phenotype that has not been described in detail, with chains of misplaced germ line meiotic nuclei spanning the rachis. These misplaced germ line nuclei were partially surrounded by germ cell plasma membrane and sheath cell projections while they were spanning the rachis. Such deep sheath cell projections in the meiotic zone were never observed in wild-type animals. The TEM cross-sections indicated that the organization of *fli-1* mutant germ line meiotic zone resembles the wild-type germ line mitotic zone (no rachis was formed and DTC projections extended into the interior of gonad).

The Glm phenotype observed in *fli-1* mutants is due to defects in the germ line but not in the sheath cells, since male *fli-1* animals, lacking the sheath cells, also displayed the same Glm phenotype and no expression of *fli-1* promoter was observed in the sheath cells. When misplaced germ line nuclei invaginate into the rachis, the sheath cells may form adhesion structure with the germ cell plasma membrane surrounding the misplaced germ line nuclei and extend into the internal

part of the gonad. As discussed before, these chains of misplaced nuclei moved proximally while associated with sheath cell projections. It is still unknown how the sheath cells can remain associated with the misplaced nuclei while they are moving. More investigations are needed to analyze the role of sheath cells in this Glm phenotype.

Germ cell morphogenesis is sensitive to gene dosage. The *fli-1(ky535)* mutation was an incomplete loss-of-function mutation, and the *fli-1(tm362)* deletion allele was a potential null allele. Heterozygotes for either mutation displayed the germ line phenotype, indicating that *fli-1* is haploinsufficient and that a precise dosage of FLI-1 is required for normal development. *let-60 Ras* was also haploinsufficient, as heterozygous *let-60 Ras* loss-of-function mutations displayed the germ cell phenotype. Mutations in *let-60 Ras* and other canonical Ras pathway components cause a failure of meiotic pachytene nuclei to progress to diakinesis upon reaching the gonad flexure, resulting in pachytene nuclei in the proximal gonad past the flexure. This phenotype was not apparent in *fli*-1 mutants.

These data suggest that *fli-1* affects germ line morphogenesis without affecting meiotic progression or other aspects of germ line differentiation. However, *fli-1(ky535)* was a hypomorph and *fli-1(tm362)* homozygotes arrested in embryogenesis before germ line development (the germ cell phenotype was scored in *fli-1(tm362)* heterozygotes). All *fli-1* genotypes in which the Glm phenotype was scored had some *fli-1* activity, so it is possible that complete loss of *fli-1* activity in the germ line would affect other aspects germ line development (e.g. meiotic progression to diakinesis similar to *let-60 Ras* or other aspects of meiotic differentiation).

FLI-1 and LET-60 Ras act together to control germ line morphogenesis. All loss-of-function alleles and dominant-negative alleles of *let-60* Ras we scored displayed the same Glm phenotype as *fli-1(ky535)*, but not the constitutively-active alleles of *let-60* Ras. Moreover, constitutively-active *let-60* Ras alleles suppressed the Glm phenotype of *fli-1* mutants, suggesting that LET-60 Ras and FLI-1 function together in controlling the germ line morphogenesis. However, these results cannot distinguish whether *let-60* and *fli-1* function through the same pathway or parallel pathways. Further genetic analyses are necessary to discriminate these two possibilities. Since the LRRs of FLI-1 bind to human Ha-Ras, this favors the model that LET-60 Ras and FLI-1 act in the same pathway.

Mutations in *sem-5, sos-1, mpk-1, lin-1, lin-25, and sur-2* all displayed the Glm phenotype, but mutations in *lin-3* and *let-23* did not. These data indicate a distinct ligand-receptor complex is used to activate the *let-60* Ras signaling pathway in controlling the germ line morphogenesis. Interestingly, LIN-3 and LET-23 are not involved in Ras function in germ line meiotic progression to diakinesis. Possibly, the Ras pathway links to a distinct ligand-receptor complex in the control of germ line morphology and meiotic progression.

FLI-1 may function in cytoplasm and/or nucleus to control germ line morphology. The experiments described here suggest that LET-60 Ras acts together with FLI-1 to control germ line morphology. LET-60 Ras acts in the cytoplasm and FLI-1 N-terminus LRRs physically bind with LET-60 Ras. Possibly, FLI-1 also acts in the cytoplasm. Once FLI-1 is activated by LET-60 Ras, it might function through LET-60 Ras pathway and/or a parallel pathway to

control germ line morphology (Figure 2.18A). Alternatively, FLI-1 may act in the nucleus. Human Flightless-1, along with a G-actin monomer, is a component of a transcriptional coactivator complex that acts with nuclear hormone receptors. Full-length *fli-1::gfp* expression was associated with germ line nuclei detected by anti-GFP antibody. In addition, FLAP might assist FLI-1 translocation by forming complex with FLI-1. These data suggest that FLI-1 may translocate into nucleus and regulate gene expression. More experiments will be required to answer these questions.

In wild-type animals, as germ line nuclei develop from mitosis to meiosis, they reorganize to the cortex of gonad and form a nucleus-free rachis. The experiments described here suggest that FLI-1 and LET-60 Ras act together to control this coordination of germ line nuclei meiotic differentiation and rachis organization. The LET-60 Ras canonical signaling pathway is also involved in control this coordination process. However, a distinct ligand-receptor complex is necessary to activate LET-60 pathway in germ line to perform this function. LET-60 Ras is also suggested to control germ line nuclei meiotic progression (from meiotic pachytene to diakinesis). So far, no evidence is found to support that FLI-1 regulates this event. Possibly, FLI-1 acts in the morphogenesis pathway with LET-60 Ras but not in the meiotic differentiation pathway. Further studies will address this idea as well as the molecular mechanisms of FLI-1 and LET-60 Ras in germ line morphogenesis.

Figure 2. 1

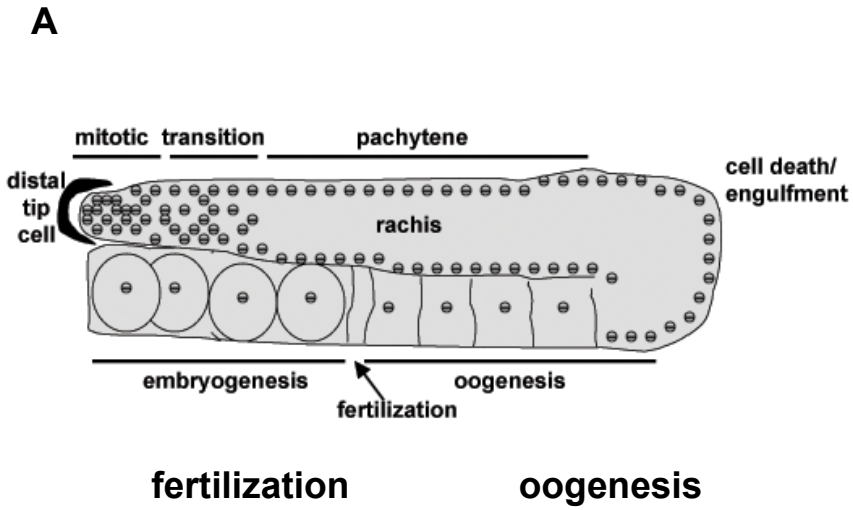
A
mitotic
transition
pachytene
distal
tip
cell
rachis
cell death/
engulfment
embryogenesis
oogenesis
fertilization
fertilization
oogenesis
B
mitotic
transition
pachytene
rachis

Figure 2. 1 Schematic diagram of wild-type *C. elegans* germ line and *fli-1(ky535)* mutant germ line. (A) shows a single hermaphrodite gonad arm. Germ line nuclei with stem cell character are located in the distal tip (mitotic zone) of gonad. Distal tip cell (DTC) functions as a stem cell niche and covers the distal tip mitotic zone. Differentiated germ line nuclei are generated by the germ line stem cells and develop from the distal tip region to the proximal gonad. When germ line nuclei migrate out from the transition zone, they develop into meiotic pachytene stage and move to the cortex of the gonad, leaving a nucleus-free rachis. When reaching the flexure region of the gonad, some of the nuclei undetgos apoptosis while the others begin oogenesis. (B) shows the phenotype of *fli-1(ky535)* mutant gonad arm. In *fli-1(ky535)* mutant germ line, instead of forming nucleus-free rachis, there are numerous chains of nuclei spanning the rachis.

Figure 2. 2

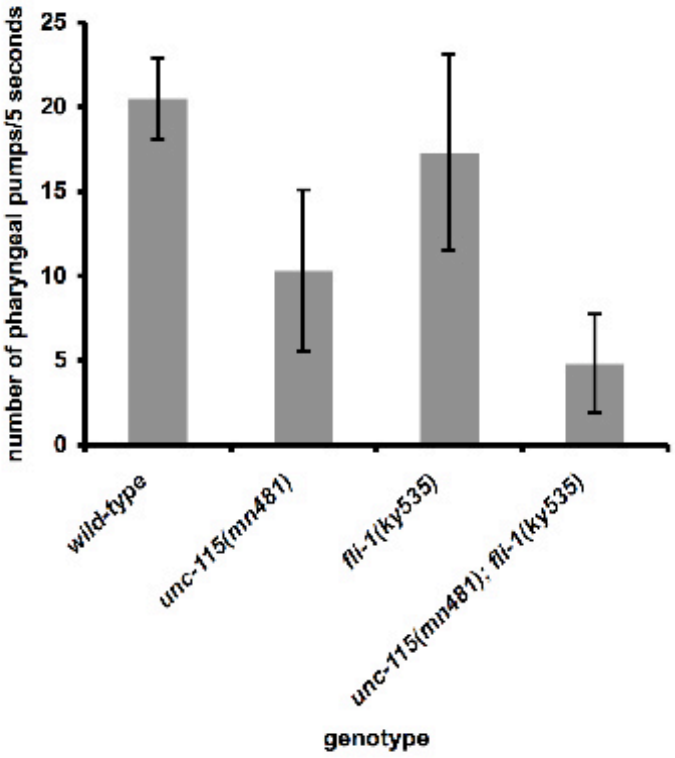
number of pharyngeal pumps/5 seconds
25
20
15
10
5
0
wild-type
unc-115(mn481)
fli-1(ky535)
unc-115(mn481); fli-1(ky535)
genotype

Figure 2. 2 Quantitative data of pharyngeal pumping defects in *unc-115(mn481), fli-1(ky535)* and *unc-115(mn481); fli-1(ky535)* mutants. The x axis consists of mutations studied, and the y axis plots the number of pharyngeal pumping times in every 5 seconds. The *C. elegans* pharynx functions like a muscular pump. In feeding animals, the open-close movement of pharynx is easily observed under DIC. In this study, L1 animals of different mutations were analyzed under DIC with plenty of food. For wild-type animals, in every 5 seconds, the pharynx pumps 21 times on average. *unc-115(mn481)* animals reduce the pharyngeal pumping movement to almost half of the wild-type rate. In *fli-1(ky535)* mutants, slight defects in pharyngeal pumping is observed. However the *unc-115(mn482); fli-1(ky535)* animals exhibit severe pharyngeal pumping defects and this lead to the lethality of these double mutant animals.

Figure 2. 3

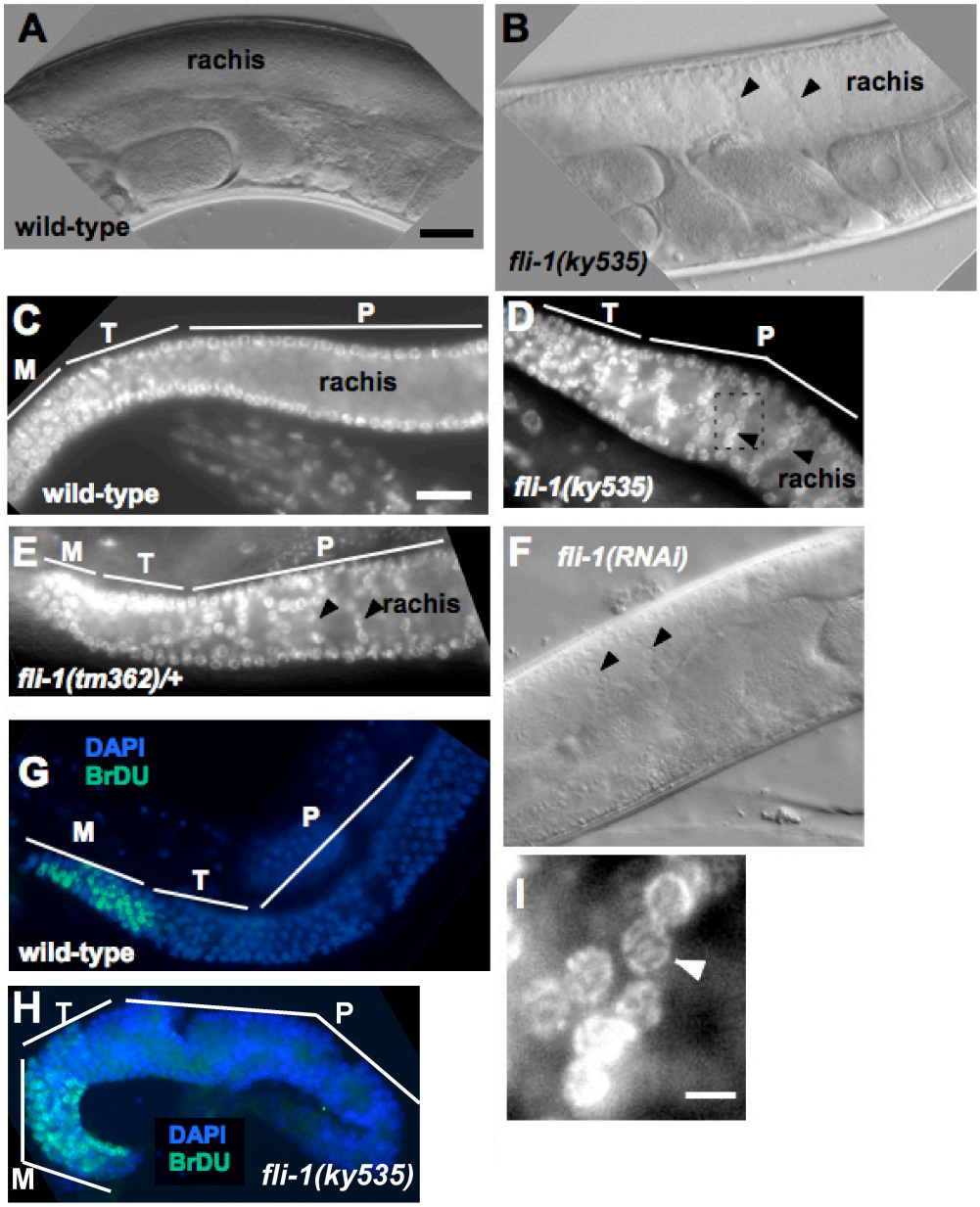
A
rachis
wild-type
B
rachis
fli-1(ky535)
C
T
P
M
rachis
wild-type
D
T
P
fli-1(ky535)
rachis
E
M
T
P
rachis
fli-1(tm362)/+
F
fli-1(RNAi)
G
DAPI
BrDU
M
P
T
wild-type
I
H
T
P
DAPI
BrDU
M
fli-1(ky535)

Figure 2. 3 *fli-1* mutants display germ line morphogenesis defects (the Glm phenotype). In all images, the distal tip of the gonad is to the left. In images (C), (D), (G), (E), and (H), the approximate extents of mitoic zones (M), transition zones (T), and meiotic pachytene zones (P) are indicated. (A) and (B) Differential Interference Contrast (DIC) images of wild-type and *fli-1(ky535)* gonads. A wild-type gonad had a germ nucleus-free rachis in the meiotic zone whereas a *fli-1(ky535)* animal displayed chains of nuclei crossing the rachis (arrowheads in (B)). (C-E). Epifluorescence images of DAPI-stained gonads from wild-type, *fli-1(ky535)*, and *fli-1(tm362)/+* animals. Wild-type shows a nucleus-free rachis, whereas *fli-1(ky535)* and *fli-1(tm362)/+* displayed chains of nuclei crossing the rachis (arrowheads). The area in dashed box in (D) is shown at a higher magnification in (I). (F) DIC image of a gonad from a wild-type animal subject to *fli-1* RNAi. Arrowheads indicate nuclei in the rachis. (G) and (H) Gonads from wild-type and *fli-1(ky535)* fed BrDU-containing bacteria for 10 minutes and fixed and stained with DAPI and anti-BrDU antibody. Nuclei in the mitotic zone of both wild-type and *fli-1(ky535)* accumulated BrDU. No BrDU-positive nuclei were seen in the meiotic pachytene regions, including the misplaced nuclei in *fli-1(ky535* (I) A magnified biew of the dashed box in (D). Misplaced nuclei show meiotic morphology as determined by DAPI staining. The scale bar in (A) = 10mM for (A-H). The scale bar in (I) = 2mM.

Firgur 2. 4

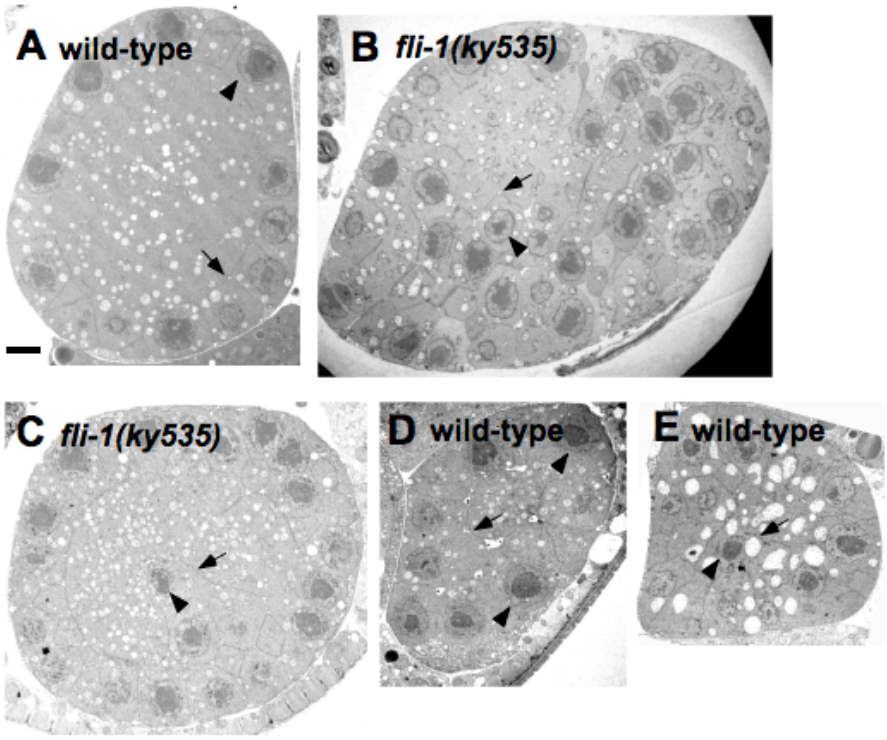

Figure 2. 4 Misplaced nuclei in *fli-1(ky535)* are partially surrounded by germ cell plasma membrane. Shown are transmission electron microscopy cross-sections of gonads from wild-type (A, D, and E) and *fli-1(ky535)* (B and C). (A) A cross-section through the meiotic pachytene zone of wild-type. The nuclei are arranged at the cortex (the arrowhead indicates a nucleus) and are partially surrounded by germ cell plasma membrane, forming the characteristic "T" structure (arrow). (B and C) Cross sections through the meiotic pachytene zone of a *fli-1(ky535)* mutant. Misplaced nuclei are apparent (arrows), and misplaced nuclei are surrounded by germ cell plasma membrane in a manner similar to nuclei at the cortex (internal "T" structure-like membrane organization is indicated by the arrows). (D and E) Cross-sections through the distal mitotic zone on wild-type. Nuclei are not arranged exclusively at the cortex (arrowhead in (E). Arrows indicate membrane surrounding internal mitotic nuclei. The scale bar in A = 2mM for all micrographs.

Figure 2. 5

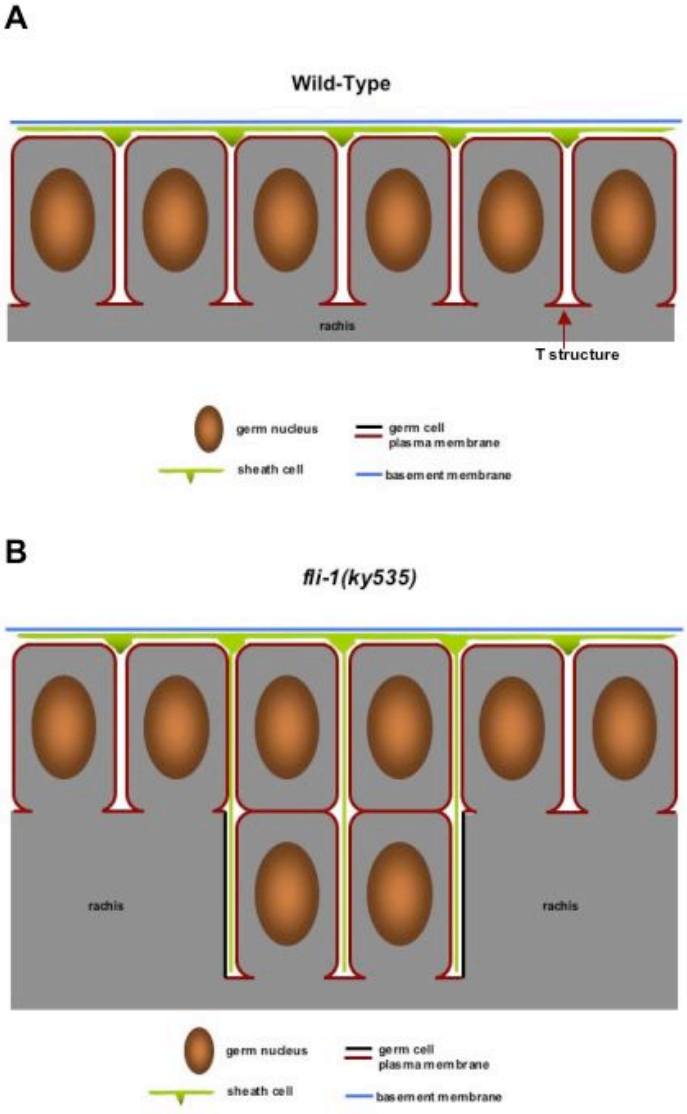
A
Wild-Type
rachis
T structure
germ nucleus
germ cell plasma membrane
sheath cell
basement membrane
B
fli-1(ky535)
rachis
rachis
germ nucleus
germ cell plasma membrane
sheath cell
basement membrane

Figure 2. 5 Schematic diagram of membrane structure that covers the germ line. *C. elegans* germ line is a syncytium with multiple germ line nuclei sharing the common cytoplasm and each of these nuclei is partially covered by membrane structure. (A) In wild-type germ line, each nucleus is partially covered by germ cell plasma membrane and the germ cell plasma membrane protrudes between each nucleus and forms the "T" structure (arrow). Part of the germ line is further covered by somatic sheath cells, which extend projections into the gaps in between of each nucleus. These projections never extend into the interior of gonad in wild-type background. The entire gonad is further enveloped by basement membrane. (B) In *fli-1(ky535)* mutants, the misplaced germ line nuclei are still attached with germ cell plasma membrane while spanning the rachis. At the same time, projections for somatic sheath cells also extend further into the interior rachis.

Figure 2. 6

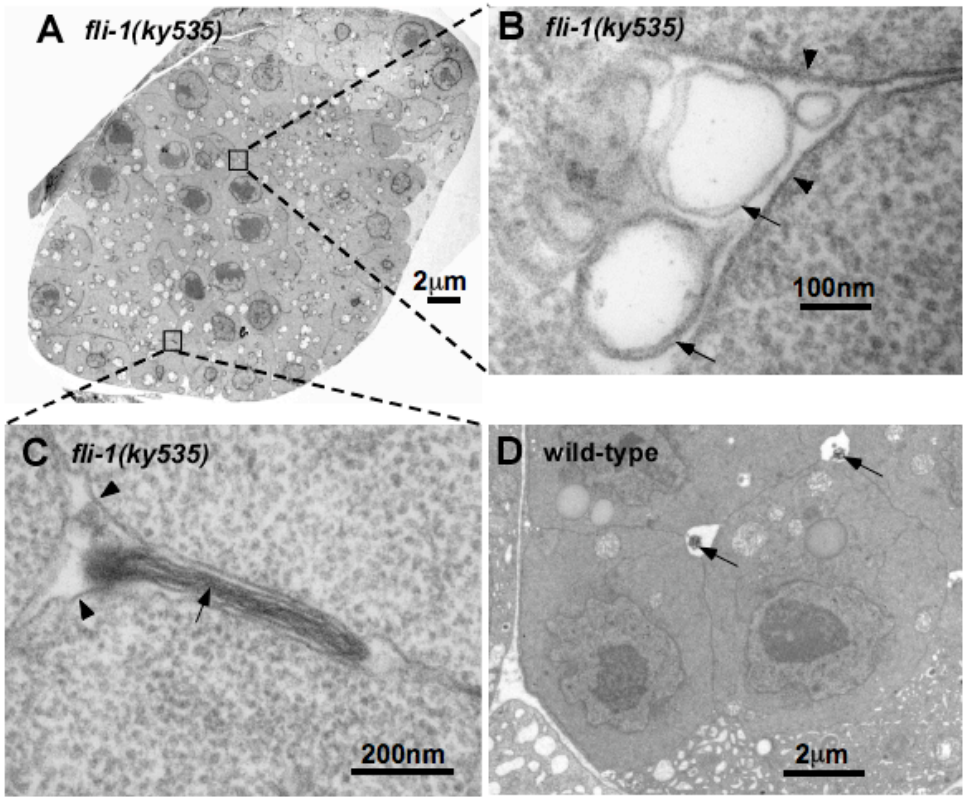
A fli-1(ky535)
2μm
B fli-1(ky535)
100nm
C fli-1(ky535)
200nm
D wild-type
2μm

Figure 2. 6 Membrane-like structures are present between misplaced germ line nuclei in *fli-1(ky535)*. (A-C) are transmission electron microscope cross-sections in the meiotic pachytene zone of *fli-1(ky535)* mutants. (D) is a section through the distal mitotic region of wild-type. (A) *fli-1(ky535)* displays misplaced nuclei and associated germ cell plasma membrane. (B and C) Higher-magnification views of regions bewteen the germ cell plasma membrane (arrowheads) surrounding misplaced nuclei. Arrows indicate membrane-like structures in the interstices between germ cell plasma membrane. The electron-dense laminar structure in (C) resembles a gap junction seen between gonadal sheath cells on the surface of the gonad. (D) A cross section through the distal mitotic zone of wild-type. Arrows indicate membrane-like structures in the germ cell plasma membrane interstices that are likely filopodia from the distal tip cell.

Figure 2. 7

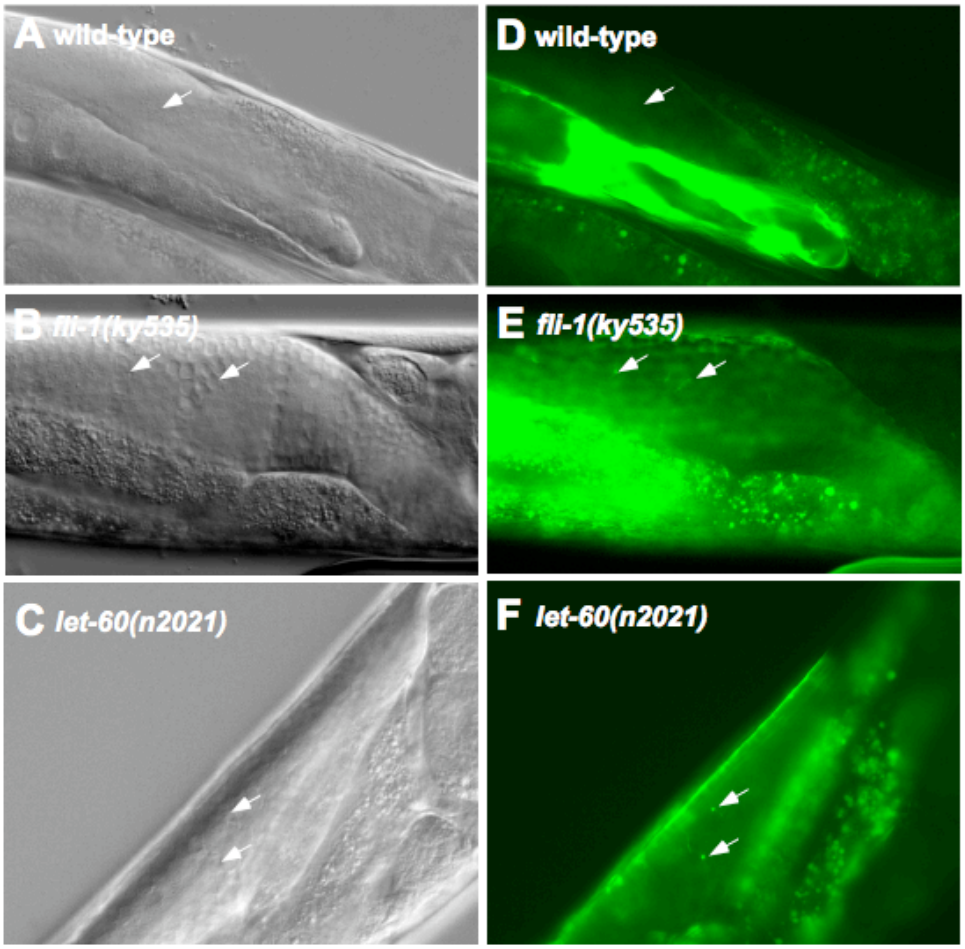
A wild-type
D wild-type
B fli-1(ky535)
E fli-1(ky535)
C let-60(n2021)
F let-60(n2021)

Figure 2. 7 Sheath cell protrusions are associated with misplaced nuclei in *fli-1(ky535)*. DIC images (A, B, and C) and fluorescence images (E, F, and G) of the meiotic zones of wild-type, *fli-1(ky535)*, and *let-60(n2021)* gonads from the same animals. The arrows in (A) and (D) point to the nucleus-free rachis in wild type. The arrows in (B) and (C) point to misplaced nuclei in *fli-1(ky535)* and *let-60(n2021)* and associated regions of *lim-7::gfp* in (E) and (F).

Figure 2. 8

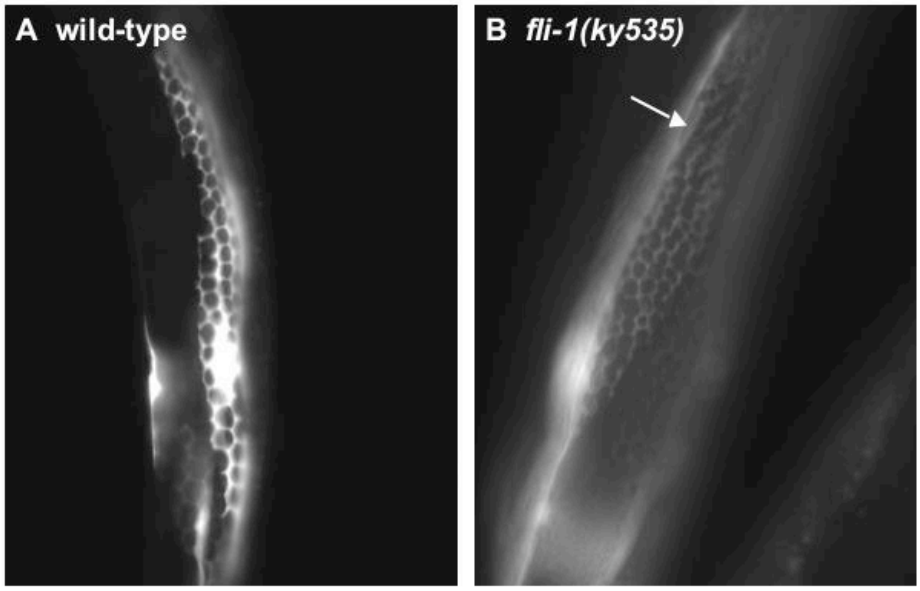

Figure 2. 8 Gonad cortex view of p*lim-7::gfp* expression in the somatic sheath cells. Somatic sheath cells partially cover the gonad and extend projections fill the gaps in between of each germ line nucleus. p*lim-7::gfp* expresses is detected in the somatic sheath cells and form a honeycomb pattern on the surface of the wild-type gonad (A). However, in *fli-1(ky535)* mutant, this honeycomb expression pattern is disorganized, indicating cortical nuclei are disorganized.

Figure 2. 9

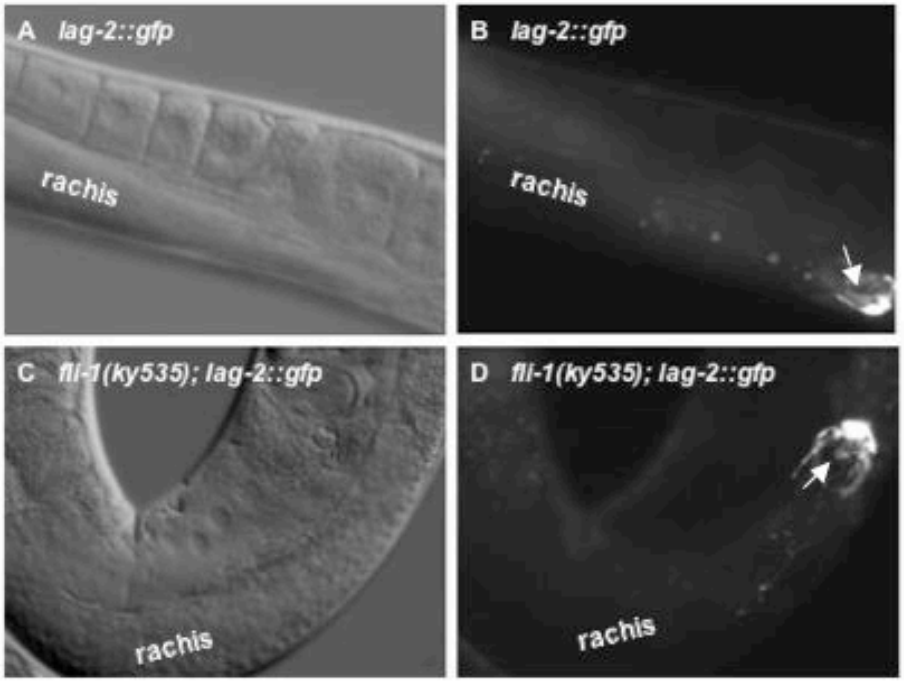
A lag-2::gfp
rachis
B lag-2::gfp
rachis
C fli-1(ky535); lag-2::gfp
rachis
D fli-1(ky535); lag-2::gfp
rachis

Figure 2. 9 *lag-2::gfp* expression in the distal tip cell of wild-type and *fli-1(ky535)* mutant animals. *lag-2::gfp* only expressed in the distal tip cell, which extend protrusions into the distal tip part of the gonad to regulate germ line stem cell proliferation. (A) is the DIC view of wild-type gonad and (B) is the GFP view of *lag-2::gfp* expression in this wild-type gonad. The protrusions from DTC are clearly visualized (arrows), but no such extensions are visualized in the pachytene zone of wild-type gonad. (C) and (D) are DIC view and GFP view of *lag-2::gfp* expression in *fli-1(ky535)* mutant gonad. Protrusions are only observed in the distal tip region of *fli-1(ky535)* gonad but not the pachytene zone. These observations suggest that distal tip cell protrusions are not associated with the misplaced germ line nuclei in *fli-1(ky535)* mutants.

Figure 2. 10

A

	nucleus diameter (μM)	nuclei/ cross-section	nuclei at cortex/cross-section
wild-type	3.0± 0.6 n=74	15.4 ± 1.9 n=8	15.4 ± 1.9 n=8
ky535	2.9± 0.6 n=101	22.6 ±6.7 n=7	16.6 ±3.0 n=7

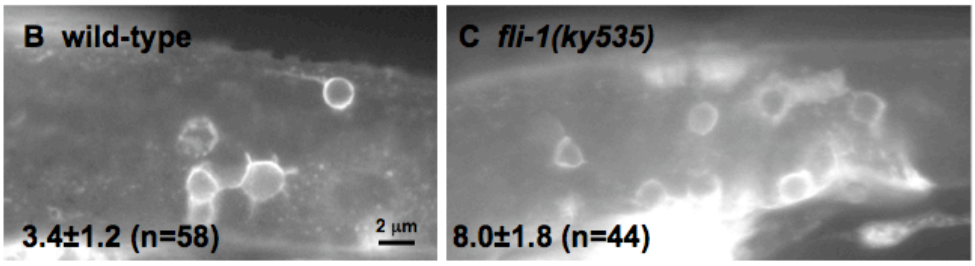

Figure 2. 10 Quantitative data suggest that *fli-1(ky535)* mutant does not affect the size of germ line nuclei but increases the apoptosis. (A) The meiotic nuclei in *fli-1(ky535)* mutant are roughly the same size as those in wild-type animals, including the misplaced germ line nuclei in the rachis. These data are obtained by measuring nuclei on TEM cross-sections. Although same number of germ line nuclei are observed on the cortex of each TEM cross-section, more germ line nuclei exist in the *fli-1(ky535)* TEM cross-section than in wild-type which can be explained by the misplaced nuclei in the rachis. (B) and (C) show the GFP-tagged CED-1 expression in the somatic sheath cells, which clustered around the nuclei undergoing apoptosis. More nuclei are observed undergoing apoptosis in *fli-1(ky535)* gonad flexure (C) than wild-type gonad (B).

Figure 2. 11

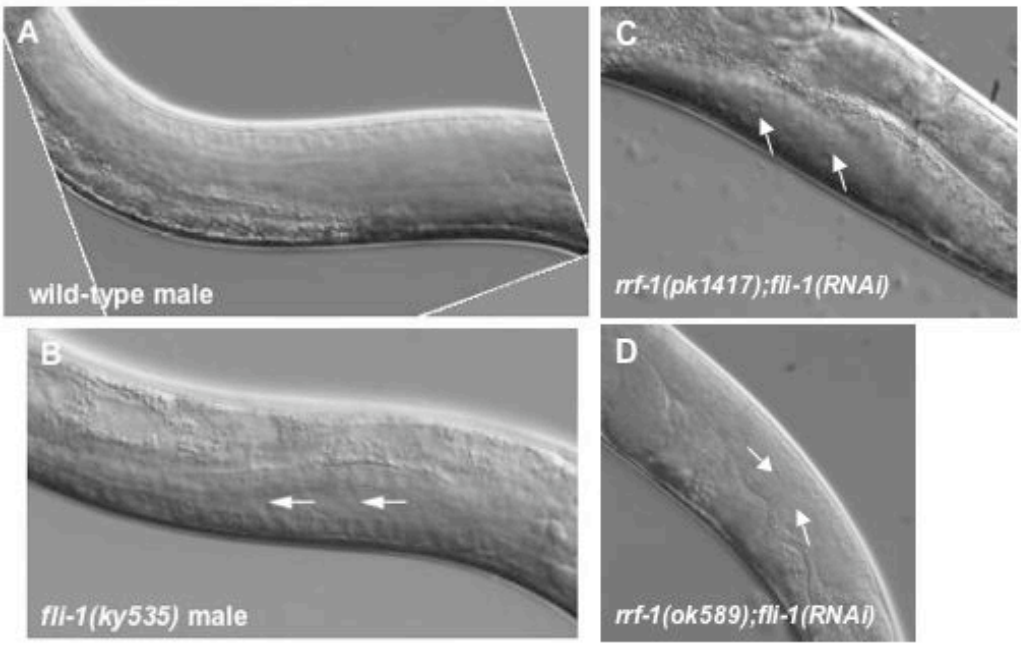
A
wild-type male
C
rrf-1(pk1417);fli-1(RNAi)
B
fli-1(ky535) male
D
rrf-1(ok589);fli-1(RNAi)

Figure 2. 11 The Glm phenotype observed in *fli-1(ky535)* mutant might be autonomous to the germ line. Pictures are showing the DIC view of wild-type male germ line (A), *fli-1(ky535)* mutant male germ line (B), *rrf-1(pk1417):fli-1(RNAi)* animal germ line (C) and *rrf-1(ok589);fli-1(RNAi)* animal germ line (D). In wild-type male gonad, germ line nuclei always associate with cortex and no misplaced nuclei can be detected inside the rachis (A). However, chains of misplaced nuclei are visualized in the rachis of *fli-1(ky535)* male germ line (B) (arrows). This suggests that *fli-1(ky535)* male animals also display the same Glm phenotype as hermaphrodites, although males do not contain somatic sheath cells. *rrf-1* mutants are sensitive to germ line RNAi but not the somatic tissue RNAi. However, *fli-1* RNAi in two *rrf-1* alleles, *pk1417* and *ok589*, produces the Glm phenotype (C and D, arrows point to chains of misplaced germ line nuclei). These observations indicate that the Glm phenotype might be autonomous to the germ line but not the somatic sheath cells.

.

Figure 2. 12

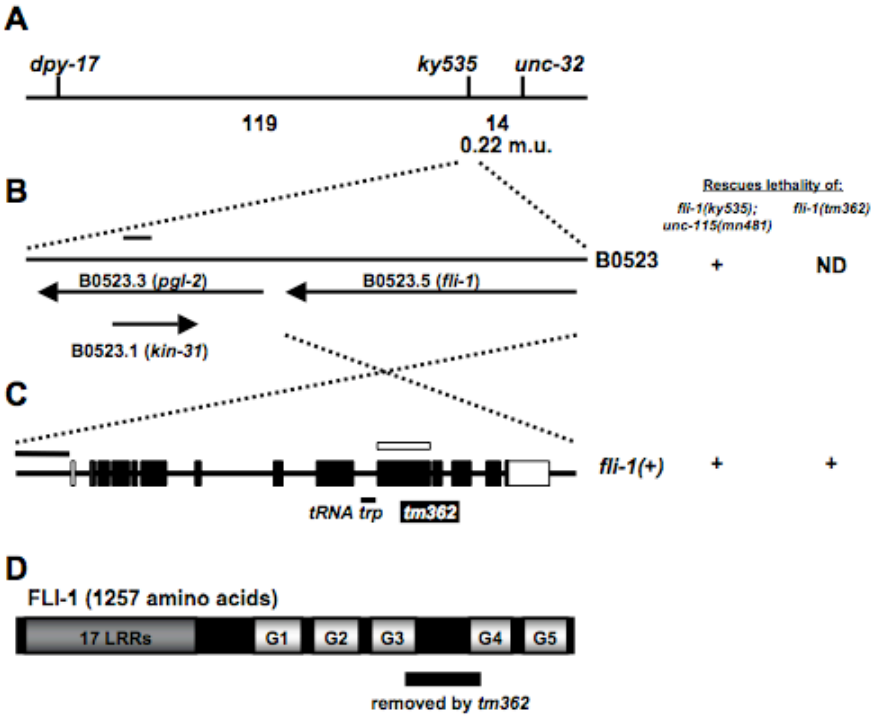
A
dpy-17
ky535
unc-32
119
14
0.22 m.u.
B
Rescues lethality of:
fli-1(ky535); unc-115(mn481)
fli-1(tm362)
B0523
+
ND
B0523.3 (pgl-2)
B0523.5 (fli-1)
B0523.1 (kin-31)
C
fli-1(+)
+
+
tRNA trp
tm362
D
FLI-1 (1257 amino acids)
17 LRRs
G1
G2
G3
G4
G5
removed by tm362

Figure 2. 12 The *fli-1* locus. (A) A genetic map of the *fli-1* region. Numbers below the line indicate the number of recombination events between the loci in three-factor crosses. The estimated genetic distance between *unc-32* and *ky535* is 0.22 map units. (B) A diagram of the cosmid B0523. Genes on the cosmid are indicated as arrows. (C) The *fli-1* gene. 5' is to the left. Black boxes indicate coding exons, and white boxes represent non-coding exons. the extent of the *tm362* deletion is indicated below the line, as is the location of a Trp tRNA gene. the white box above the line indicates the regiuon used in *fli-1* RNAi experiments, and the black line represents 1 kb. (D) A diagram of the predicted FLI-1 polypeptide. The locations of the 17 leucine-rich repeats (LRRs) and the five gelsolin-like repeats (G1-G5) are indicated. The deletion *fli-1(tm362)* removes coding region for the residues of FLI-1 indicated below the diagram.

Figure 2. 13

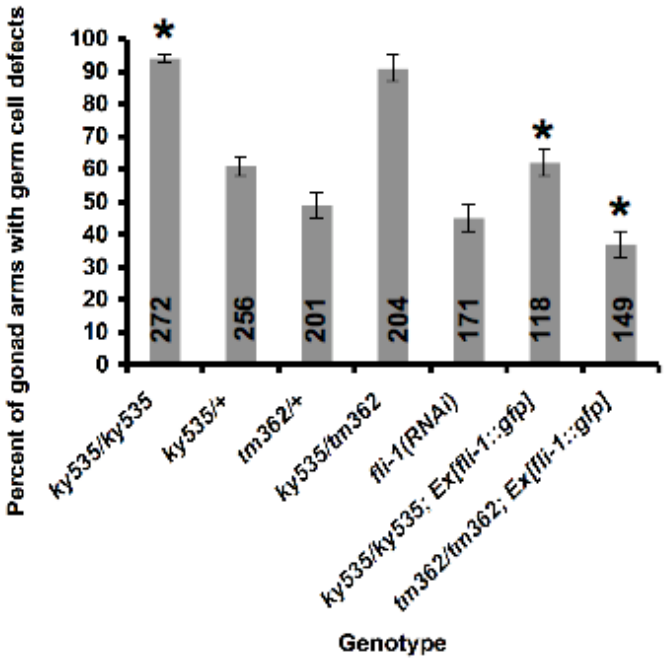
Percent of gonad arms with germ cell defects
100
90
80
70
60
50
40
30
20
10
0
*
*
*
272
256
201
204
171
118
149
ky535/ky535
ky535/+
tm362/+
ky535/tm362
fli-1(RNAi)
ky535/ky535; Ex[fli-1::gfp]
tm362/tm362; Ex[fli-1::gfp]
Genotype

Figure 2. 13 Quantitation of germ cell defects in *fli-1* mutants. Genotypes are indicated along the y axis, and percent of gonad arms displaying the germ cell morphogenesis defect is the x axis. For each genotype, the number of gonad arms scored is indicated inside the bar, and the standard error of the proportion is shown as error bars. Asterisks indicate that the differences between genotypes is significant ($p < 0.001$; t-test and Fisher's Exact analysis).

Figure 2. 14

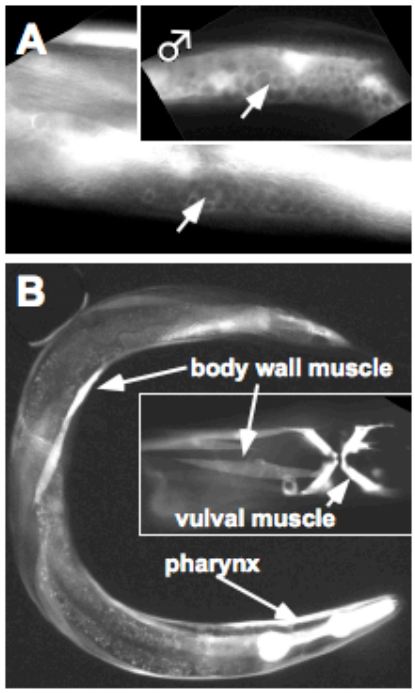

Figure 2. 14 *fli-1::gfp* is expressed in germ line and is muscle. Shown are epifluorescence images of wild-type animals harboring a transgene consisting of the *fli-1* promoter driving *gfp* expression. (A) Arrows point to germ line expression in a hermaphrodite and a male (inset). The "honeycomb" pattern is due to exclusion of GFP from the nuclei of the germ line. (B) Arrows point to *pfli-1::gfp* expression in body wall muscle, pharygeal muscle, and vulval muscle (inset).

Figure 2. 15

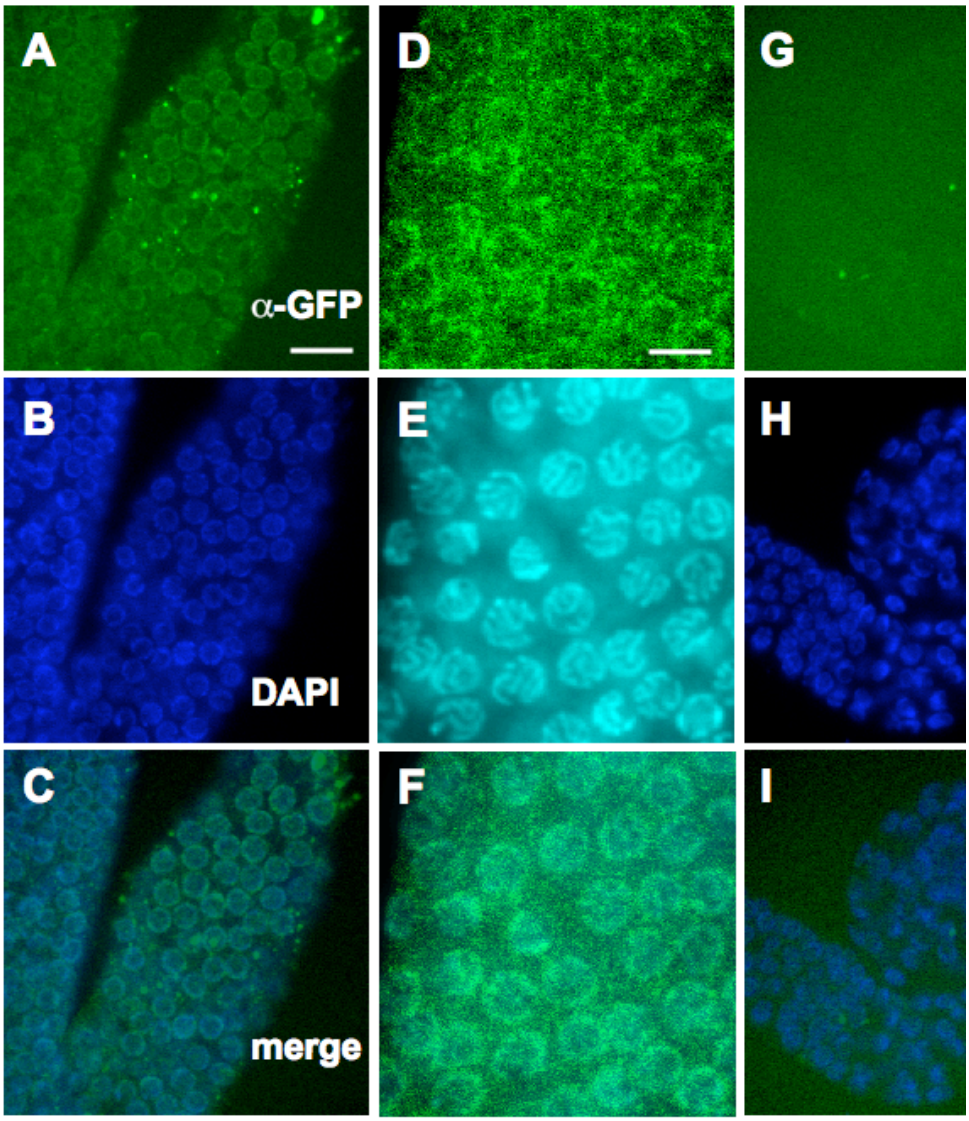

Figure 2. 15 FLI-1::GFP accumulates at nuclei. Confocal images of gonads from animals stained with anti-GFP antibody and DAPI. (A-F) are images of gonads from animals harboring the full-length *fli-1::gfp* transgene that rescues the *fli-1* Glm phenotype and that is predicted to encode a full-length FLI-1 protein tagged with GFP at the C-terminus. (G-I) are images of an animal without the *fli-1::gfp* transgene. FLI-1::GFP reactivity was found associated with germ line nuclei.

Figure 2. 16A

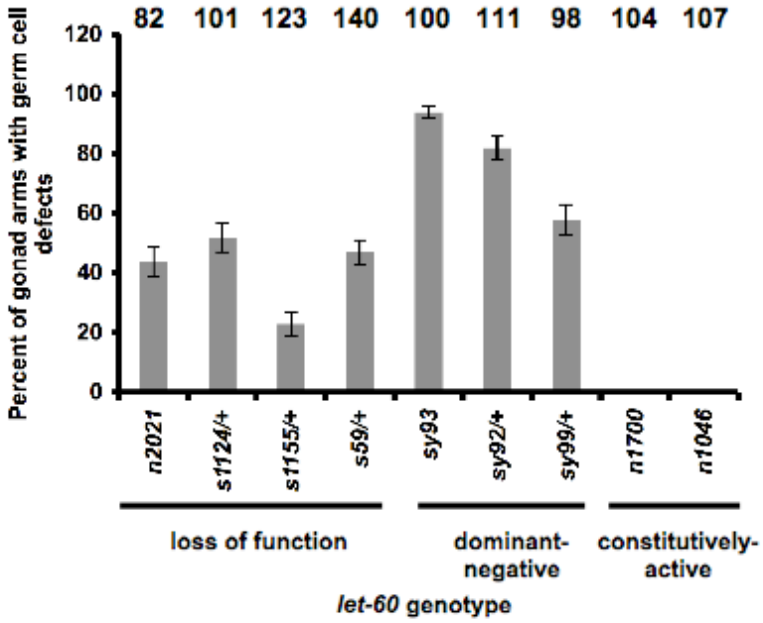
82 101 123 140 100 111 98 104 107
Percent of gonad arms with germ cell defects
120
100
80
60
40
20
0
n2021
s1124/+
s1155/+
s59/+
sy93
sy92/+
sy99/+
n1700
n1046
loss of function
dominant-negative
constitutively-active
let-60 genotype

Figure 2. 16B

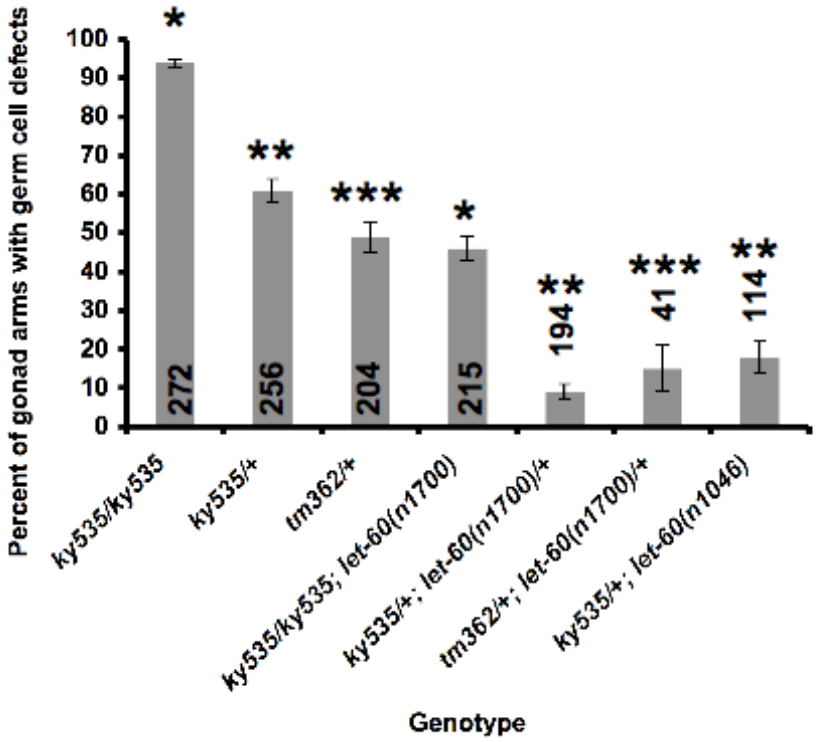
Percent of gonad arms with germ cell defects
100
90
80
70
60
50
40
30
20
10
0
*
**
***
*
194 **
41 ***
114 **
272
256
204
215
ky535/ky535
ky535/+
tm362/+
ky535/ky535; let-60(n1700)
ky535/+; let-60(n1700)/+
tm362/+; let-60(n1700)/+
ky535/+; let-60(n1046)
Genotype

Figure 2. 16 FLI-1 interacts with LET-60 Ras to control germ cell morphogenesis. Genotypes are along the x axis, and percentage of gonad arms displaying the germ cell phenotype are along the y axis. Numbers of gonads scored for each genotype are indicated. Error bars represent the standard error of the proportion, and matching numbers of asterisks indicate that the genotypes are significantly different (t-test and Fisher's Exact analysis; $p < 0.001$). (A) Loss-of-function and dominant-negative alleles of *let-60 Ras* displayed the Glm phenotype whereas constitutively-active alleles did not. (B) Two constitutively-active alleles of *let-60 Ras* suppress the Glm phenotype of *fli-1(ky535)* and *fli-1(tm362)*/+.

Figure 2. 17

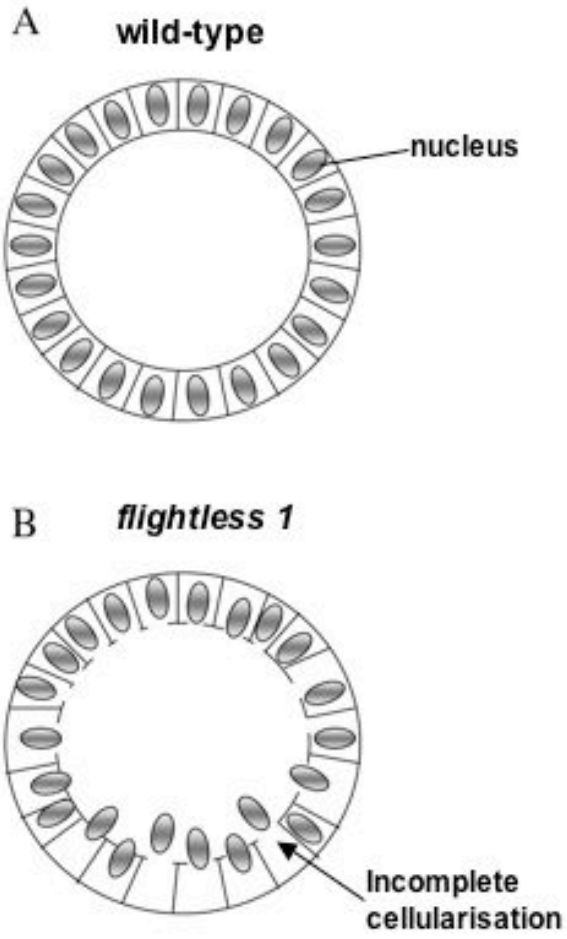
A
wild-type
nucleus
B
flightless 1
Incomplete
cellularisation

Figure 2. 17 Schematic diagrams show the defects in nuclear positioning seen in the cross-sections of *flightless* 1 mutant Drosophila embryos. Shown are cross-sections of *Drosophila* embryos: (A) wild-type, (B) *flightless 1* mutant. In wild-type *Drosophila* embryos, nuclei arranged on the peripheral surface of the egg and forming a single nucleus layer. Soon after the nuclei have begun to elongate, the cellularisation has begun (A). In *flightless 1* mutant embryo, the cellularization step is defective. As a consequence, nuclei move out of the incompletely cellularized peripheral layer of cytoplasm into the inside of the egg.

Figure 2. 18

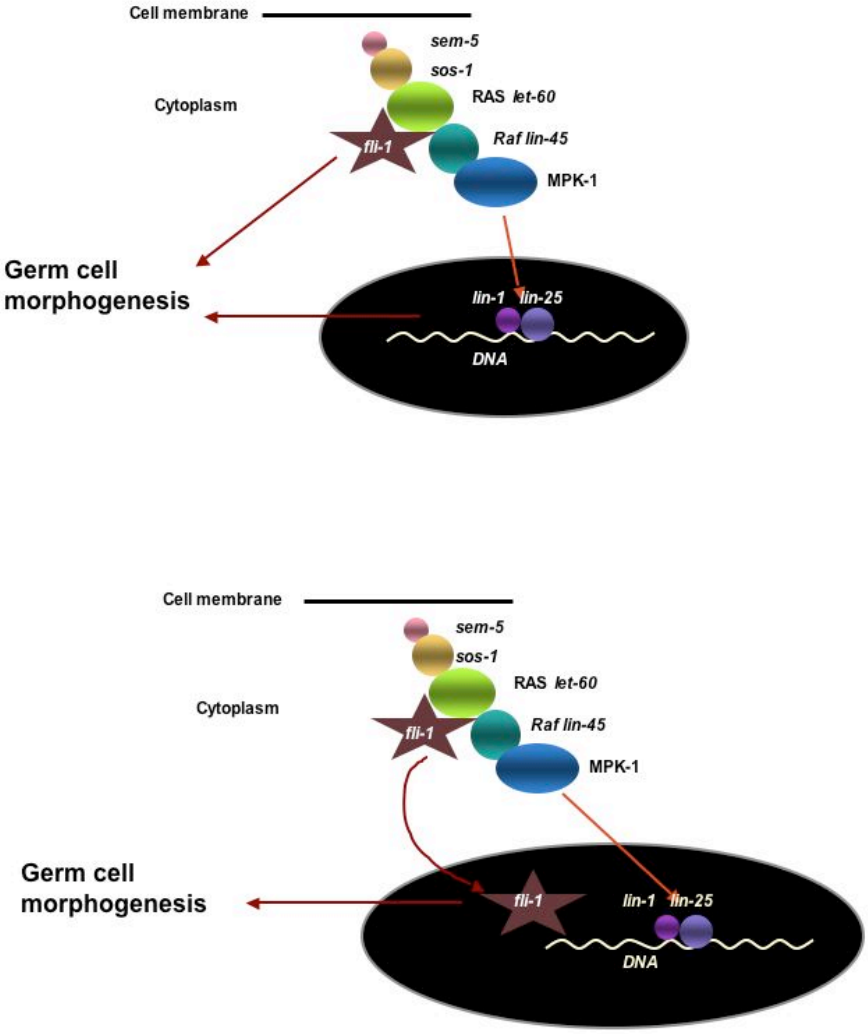
Cell membrane
sem-5
sos-1
Cytoplasm
RAS let-60
fli-1
Raf lin-45
MPK-1
Germ cell
morphogenesis
lin-1
lin-25
DNA
Cell membrane
sem-5
sos-1
Cytoplasm
RAS let-60
fli-1
Raf lin-45
MPK-1
Germ cell
morphogenesis
fli-1
lin-1
lin-25
DNA

Figure 2. 18 Function models of FLI-1 and LET-60 Ras in regulating germ line morphogenesis. (A) A distinct ligand-receptor complex may initiate the activation of LET-60 Ras signaling pathway. The activated LET-60 Ras binds and activates FLI-1. The Activated FLI-1 therefore regulates germ line morphogenesis through LET-60 pathway or a separate pathway. This model is used to explain the function of FLI-1 in the cytoplasm. (B) An alternative model can be used to explain FLI-1 function in the nucleus. After being activated by LET-60 Ras, FLI-1 may translocate into the nucleus and regulate gene expression that affects germ line morphogenesis as a consequence.

Figure 2. 19

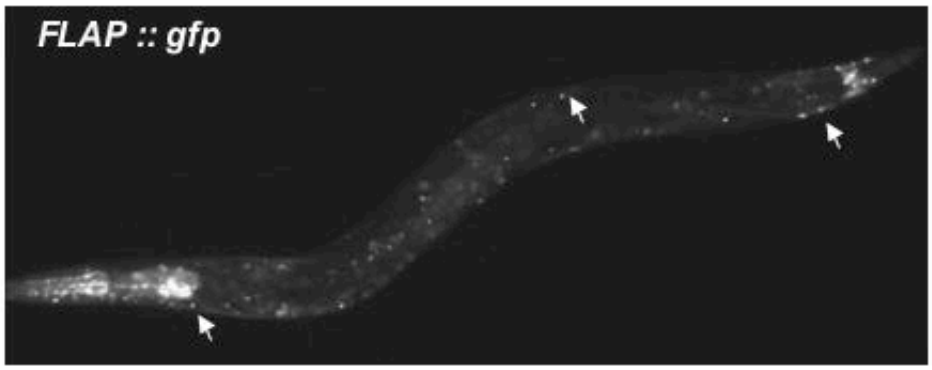

Figure 2. 19 *FLAP:: gfp* expression pattern in wild-type *C. elegans*. The full-length *FLAP:: gfp* transgene expression is observed in pharynx and body wall muscle. FLAP::GFP accumulates in nuclei of cells (arrows).

Figure 2. 20

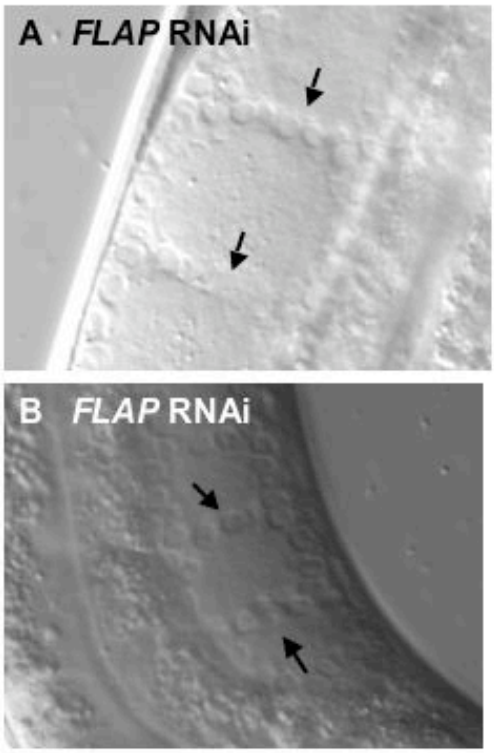

Figure 2. 20 *FLAP* RNAi animals produce Glm phenotype. (A) and (B) are showing individual *FLAP* RNAi animal. Inside the rachis, chains of misplaced germ line nuclei are observed spanning the rachis (arrows).

CHAPTER III

FLI-1 regulates muscle development in *C. elegans*

3. 1. Abstract

The *fli-1* gene in *C. elegans* is a homologue of *Drosophila flightless 1*. *flightless 1* null mutant *Drosophila* embryos exhibit partial cellularization and gastrulation defects (discussed in Chapter II). Flies carrying weak alleles of *flightless 1* lack the ability to fly and display abnormal flight muscle ultrastructure. As a homologue of *Drosophila flightless 1, fli-1* gene in *C. elegans* may also play a role to control muscle development. As already discussed in Chapter II, *fli-1(ky535)* mutants had feeding defects due to malfunctional pharyngeal pumping. *fli-1*(*ky535)* and *fli-1(tm362)* animals also exhibited body wall muscle defects. *fli-1(ky535)* animals displayed disorganized myofilament lattices under TEM-cross sections and *fli-1(tm362)* embryos exhibited Pat (paralyzed arrest at embryonic two-fold stage) phenotype. These all suggest that *C. elegans* FLI-1 regulates muscle development.

3. 2. Introduction

flightless 1 mutations in the fruit fly, *Drosophila*, cause flightlessness due to defects in the indirect flight muscle. In severe cases, incomplete cellularization happens during early embryogenesis, resulting subsequent abnormalities in mesoderm invagination and in gastrulation. *Drosophila flightless 1* gene encodes an actin-binding protein and is composed of N-terminal leucine-rich repeats and C-terminal gelsolin-like domains. *flightless 1* homologous genes also exist in *C. elegans*, mouse and human. The *C. elegans* and human FLI1 proteins are 49% and 60% identical to the *D rosophila* FLI1 protein respectively, suggesting a fundamental role for this protein in many metazoans.

As discussed in Chapter II, *fli-1(ky535)* mutation in *C. elegans* caused a disorganized germ line morphology, with numerous chains of meiotic germ line nuclei spanning the rachis. This phenotype seen in *C. elegans* germ line is similar to the phenotype observed in *flightless 1* mutant embryos, where the incompletely cellularized nuclei loss their peripheral positioning and migrate to the center of the egg. This similarity indicates that other than conserved protein sequence, *fli-1* gene may play conserved functions in different organisms.

Flies carrying weak alleles of *flightless 1* display impaired ability to fly. An ultrastructural level analysis reveals that those mutant flies have defective indirect flight muscle myofibrils. This implies that *flightless 1* gene may also play a role in regulating muscle development. As a matter of fact, the human FLI1 protein is found extensively expressed in skeletal muscle, although the expression is also detected in heart, brain, placenta, lung, liver, kidney and pancreas. Does *fli-*

1 regulate muscle development in *C. elegans*? Since *fli-1* gene is highly conserved through *Drosophila, C. elegans* and human, the knowledge about FLI-1 obtained in *C. elegans* is going to improve our understanding of FLI1 functions in human.

Here we report that FLI-1 also controls muscle development in *C. elegans*. In *fli-1(ky535)* mutants, disorganized body wall muscle myofilament structure was observed by both TEM and birefringence. The *fli-1(tm362)* caused a Pat phenotype (Paralyzed Arrested at Two fold stage), suggesting severe body wall muscle defects. These results suggest that FLI-1 controls multiple aspects of development, including germ line morphogenesis and myofilament lattice structure.

3. 3 Materials and Methods

***C. elegans* strains and genetics.** *C. elegans* were cultured as described. All experiments were done at 20°C unless otherwise noted. The Bristol strain N2 was used as the wild-type. The following mutations and transgenes were used. LGX: *unc-115(mn481*. LGIII: *fli-1(ky535)*, *fli-1(tm362)*.

Imaging and microscopy. Differential Interference Contrast (DIC), polarized light, and epifluorescence images were taken using a Leica DMR compound light microscope with a Hamamatsu Orca digital camera. TEM images were collected using a Jeol transmission electron microscope with digital camera.

TEM specimen preparation. 12-hour-old adult hermaphrodite animals were fixed by a modified two-step fixation based upon previous techniques (David H. Hall, 1995). Animals were anaesthetized using 8% EtOH in M9 buffer for 5 minutes. Animals were then placed in glass well slides and marinated with fixation solution (2.5% glutaraldehyde, 1% formaldehyde in 0.1M sucrose, 0.05M cacodylate, pH7.4) on ice for 30 minutes. Animals were then cut in half using a scalpel and incubated in fixation solution overnight at 4°C. Animals were then rinsed on ice 3 times with 0.2M cacodylate for 10 minutes each, incubated with 0.5% OsO_4, 0.5% $KFe(CN)_6$ in 0.1M cacodylate for 90 minutes on ice followed by three 10-minute 0.1M cacodylate buffer washes. Specimens were stained in 1% uranyl acetate in 0.1M sodium acetate, pH 5.2, for 1 hour at room temperature, followed by three 5-minute 0.1M sodium acetate washes and three 5-minute distilled water washes. Worms were packed in parallel in a V-shaped plexiglass trough and were embedded 3% seaplaque agarose. Approximately

1mm2 blocks then were dehydrated in acetone and embedded in Embed 812 (Dentler and Adams 1992)

Cross-sections of worms were cut using a diamond knife and Leica microtome and were picked up on carbon-over-formvar coated single hole grids. Sections were dried overnight and then stained using minor modifications of the Hall (1995) procedure. Stains and washes were prepared in 16 well plastic culture dishes at room temperature. Grids were stained in 1% uranyl acetate, 50% methanol for 15 minutes, rinsed twice (30 seconds each) with 100% ethanol followed by 50% ethanol/water (15 seconds), 30% ethanol/water (15 seconds), and four 15 second washes in water. Sections then were stained for 5 minutes with 0.1% lead citrate in 0.1M NaOH, rinsed twice with 0.02M NaOH (1 minute/change), rinsed five times in water (15 seconds/wash) and were air-dried before examination with the TEM.

3. 4. Results

***fli-1::gfp* is expressed in pharyngeal muscle, body wall muscle and Vulval muscle.** *fli-1 promoter::gfp* was generated to detect the expression pattern of *fli-1*. *fli-1* promoter expression was not only observed in germ line, but also in pharyngeal muscle, body wall muscle and vulval muscle (Figure 2.14), suggesting *fli-1* also play a role in regulating muscle development in these regions. Additionally, full-length *FLAP ::gfp* was also expressed in pharyngeal muscle and body wall muscle, raising the possibility that *fli-1* has function in these regions and *FLAP* assists *fli-1* to perform its role.

***fli-1(ky535)* mutants display a weakly dumpy phenotype and abnormal body wall muscle ultrastructure.** *fli-1(ky535)* mutants displayed weakly dumpy (short and fat) phenotype observed by DIC (Figure 3.1). Wild-type adult animal's body length is about 0.98-1.08mM (n=10) and *fli-1(ky535)* adult animals are about 0.74-0.95mM in length (n=10). However these animals moved normally. This abnormal body shape could be due to irregular body wall muscle structure as body wall muscle is necessary for embryonic elongation. To further investigate the ultrastructure level changes in the body wall muscle, TEM was performed.

In vertebrate muscle, the myosin-containing thick filaments are attached to M lines and actin-containing thin filaments are attached to Z lines and this arrangement forms the basic building block of vertebrate muscle. Similar to vertebrate muscle structural unit, in *C. elegans* muscle, the myosin-containing thick filaments are attached to M lines. However, instead of Z lines, in the *C.*

elegans muscle sarcomere, actin-containing thin filaments are attached to dense bodies and these actin-containing thin filaments are organized surrounding the thick filaments. Although the vertebrate muscle and *C. elegans* muscle have similar structural units, the arrangements of these units in vertebrates and *C. elegans* are different. In vertebrate, the body wall musculature forms cross-striated array. However, in *C. elegans* body wall muscle, these structural units are arranged obliquely. This body wall muscle organization was observed on TEM cross-sections of wild-type animal (Figure 3.2A).

The disruption of this myofilament lattice was occasionally observed on the TEM cross-sections of *fli-1(ky535)* mutants (Figure 3.2B). By analyzing the TEM cross-sections of *fli-1(ky535)* mutants, at ultrastructural level, the myosin-containing thick filaments were more dramatically disorganized compared with thin filaments surrounding them. This disruption often observed only on part of a single body wall muscle spindle, with the rest of the spindle displaying normal organization. Thick filaments were no longer parallel, resulting in longitudinal sections of filaments.

The body wall muscle organization was also analyzed by birefringence. Body wall muscle can be visualized by using polarized light in living animals (Figure 3.2C-D). Under birefringence, the body wall muscle spindles of wild-type animals were composed of parallel-arranged alternating bright and dark bands. The bright bands corresponded to the regions containing thick filaments, while the dark bands represented the areas of thin filaments only, and the rows of bright dots reflected the discontinuous dense bodies (Figure 3.2C). However, in *fli-1(ky535)* mutants, the parallel-arranged thick filaments and thin filaments were

disrupted in some regions of the spindle (Figure 3.2D), which is consistent with TEM results. Possibly, the myosin-containing thick filaments fuse together in *fli-1(ky535)* mutants.

***fli-1(tm362)* homozygous animals arrest at embryo stage and display Pat (paralyzed arrest at embryonic two-fold stage) phenotype.** *C. elegans* mature oocytes become fertilized by fusion with sperm as they enter the spermatheca. After forming the zygote, the single cell starts early cleavage and gastrulation. At this stage, most of the cell proliferation is complete and cells begin to differentiate. From this time onward, the *C. elegans* embryo enters organogenesis and morphogenesis and the first muscle twitches happen shortly before two-fold stage. From two-fold stage, the embryo elongates to form three-fold stage animal. Body wall muscle is required for elongation past the two-fold stage. The three-fold stage embryo contains fully differentiated tissues and organs and ready to hatch.

fli-1(tm362) homozygous mutants arrest at several embryogenesis stages (Figure 3.3). 30% of embryos arrested at early embryogenesis, including gastrulation, indicating that *fli-1* gene may play a role in regulating early embryogenesis and this deserves further investigation. 70% of the embryos displayed the Pat phenotype. Pat phenotype is a characteristic phenotype of body wall muscle defects, since the elongation of embryos from two-fold stage to three-fold stage requires the growth and force from body wall muscle. Additionally, full-length *fli-1::gfp* construct rescued the Pat phenotype of *fli-1(tm362)* homozygous embryos (Figure) and allowed those animals to grow into adult stage, raising the possibility that *fli-1* mutations cause the body wall muscle

defects. These results are consistent with the body wall muscle defects discussed earlier in *fli-1(ky535)* mutants, suggesting that *fli-1* gene plays a role in regulating muscle development in *C. elegans* as it does in *Drosophila.*

3. 5. Discussion

As a homologue of *Drosophila flightless 1*, *C. elegans fli-1* gene is expected to regulate similar developmental processes to those occurring in *Drosophila*. The severe *flightless 1* mutant *Drosophila* embryos do not cellularize completely. As a result, the nuclei that already migrate to the cortex loose their cortical positioning and some even drop toward the centre of the egg. This phenotype observed in *Drosophila* embryos resembles the Glm phenotype detected in *fli-1* mutant *C. elegans* germ line. Flies carrying weaker *flightless 1* allele are viable, but their flight ability is impaired due to defects in the indirect flight muscles. Ultrastructural analysis reveals disorganized myofibrils in the indirect flight muscles of these flies. Muscle defects are also observed in *fli-1(ky535)* and *fli-1(tm362)* mutant *C. elegans.*

***C. elegans* carrying *fli-1* mutations, *ky535* and *tm362*, display body wall muscle defects.** *fli-1(ky535)* mutants were viable, with slightly dumpy body shape. Ultrastructural level TEM cross-sections revealed disorganized myofilaments of body wall muscle. In addition, birefringence analysis detected similar myofilament lattice disorganization. Another deletion allele of *fli-1*, *tm362*, was homozygously lethal. 70% of tm362 embryos arrested at two-fold stage of embryogenesis, displaying Pat phenotype. This Pat phenotype is due to defects in the body wall muscle, which make the two-fold embryos fail to elongate into three-fold stage. With the expression of a full-length *fli-1::gfp* transgene, *fli-1(tm362)* homozygous embryos restored the ability to elongate and developed into adult stage, indicating that wild-type copy of *fli-1* gene can

specifically rescue the body wall muscle defects in those mutant embryos. The experiments described here suggest that *Drosophila flightless 1* homologue *fli-1* maintains a functional similarity in regulating muscle development as does in *Drosophila*.

***fli-1* gene might play a role in early embryogenesis.** Beside the embryos arrested at two-fold stage, 30% of *fli-1(tm362)* embryos died at earlier embryogenesis stage, gastrulation. This single piece of datum suggests *fli-1* gene may function to regulate earlier embryogenesis events in addition to muscle development. More examinations are needed to explore the function of *fli-1* in early embryogenesis.

***pfli-1::gfp* is expressed in vulval muscles and pharyngeal muscles.** *fli-1(ky535)* animals displayed feeding defects as discussed in chapter II. In addition, *pfli-1::gfp* was also observed in the vulval muscles, but no vulval defects were observed in neither *fli-1(ky535)* mutants nor *fli-1(tm362)/+* mutants so far. Further analyses are necessary to detect the subtle defects in vulval muscles. Since *fli-1* function is possibly dosage dependent, it is possible that the remaining *fli-1* activity is enough to keep vulval muscles function normally in those mutants. In the meanwhile, genes that are redundant to *fli-1* also contribute to the normal development of vulval.

In addition to the germ line defects presented in Chapter II, *fli-1* mutants also displayed muscle defects. It is not known that through which pathway FLI-1 controls muscle development. The experiments described here are still preliminary. To obtain a profound understanding of FLI-1 function in the muscles, a more careful analysis will be required.

Figure 3. 1

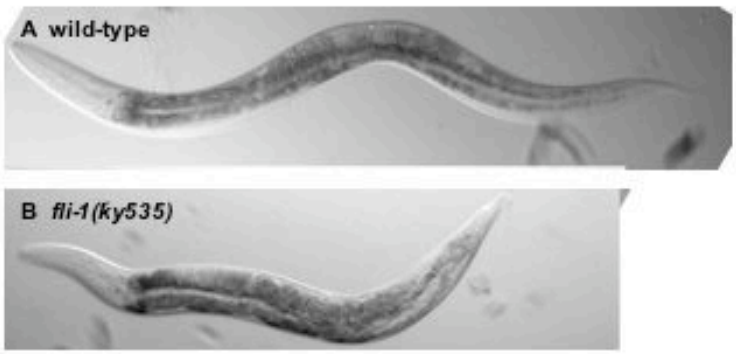

Figure 3. 1 *fli-1(ky535)* mutant animals are slightly dumpy (short and fat). (A) and (B) are DIC images of adult wild-type animal and *fli-1(ky535)* animal respectively. Comparing the body length of wild-type and *fli-1(ky535)* mutant, *fli-1(ky535)* animals are slightly dumpy.

Figure 3. 2

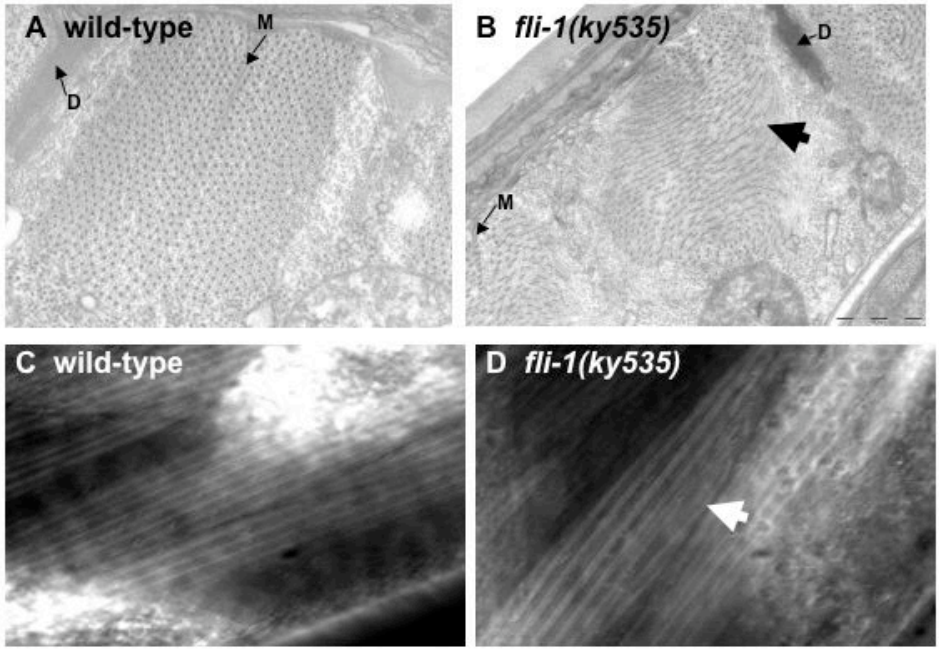

Figure 3.2 *fli-1(ky535)* mutants have disorganized body wall muscle structure. (A) On wild-type TEM cross-sections, the body wall muscle structure is very well maintained. “D” indicates the position of dense body and “M” indicates the M line. Bigger dots represent the myosin containing thick filaments surrounded by actin containing thin filaments (small dots). The thick filaments and thin filaments structures are disrupted in *fli-1(ky535)* mutant body wall muscle. As seen on *fli-1(ky535)* TEM cross-sections (B), the regular body wall muscle is disorganized (arrow) in part of a single body wall muscle cell, but the rest part of the cell is normal. Similar disorganized body wall muscle is also observed under birefringence (C, D). Body wall muscle spindles are visualized under birefringence. In wild-type animals (C), thick filament containing region (thick lines) and thin filament containing region (thin lines) are arranged in parallel. However when *fli-1(ky535)* animals are examined under birefringence (D), partially disorganized body wall muscle spindles are detected occasionally.

Figure 3.3

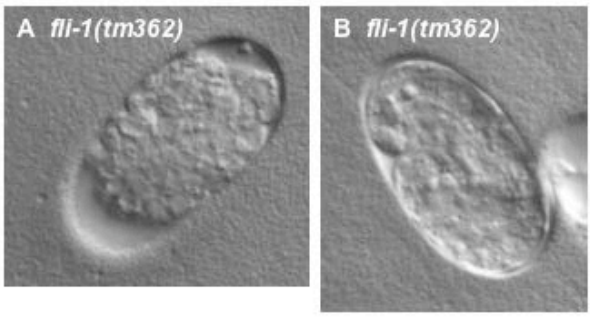

Figure 3.3 *fli-1(tm362)* homozygous animals arrest at embryogenesis stages. *fli-1(tm362)* mutation is homozygously lethal. Further analysis reveals that 30% of the *fli-1(tm362)* homozygous embryos arrest at early embryogenesis (A), while the other 70% of these embryos arrest at two-fold embryogenesis stage (B), exhibiting Pat phenotype. For embryos showing Pat phenotype, they have already developed pharynx, but due to the severe defects in the body wall muscle, they cannot elongate into three-fold stage and rather arrested at two-fold stage.

CHAPTER IV

FLI-1 affects germ line tumor formation in *C. elegans*

4. 1. Abstract

We have shown that an actin-binding protein, FLI-1, regulates germ line morphogenesis and muscle development in *C. elegans*. To further explore the functions of FLI-1 in germ line, the interaction of *fli-1* gene and *gld-1* gene was studied. *gld-1* gene encodes a STAT/KH domain containing RNA binding protein, which is required to maintain meiotic stage of germ line nuclei in the pachytene region of the gonad. In *gld-1(q485)* animals, the meiotic germ line nuclei re-enter mitosis at the proximal region of the gonad, and excess mitotic nuclei fill the germ line and form a germ line tumor. Here we reported that this germ line tumor in *gld-1(q485)* animal was slightly repressed by *fli-1(ky535)* mutation. Additional data suggest that this repression may due to the abilities of *fli-1(ky535)* mutation to increase apoptosis and to delay meiotic germ line nuclei re-entering mitosis.

4. 2. Introduction

How germ line nuclei develop from mitosis to meiosis and maintain the pachytene stage in *C. elegans* germ line is a major question in germ line research. It is known that the LIN-12/Notch family receptor GLP-1 protein is expressed only on the mitotic distal tip region of the gonad. GLP-1 acts as a receptor for LAG-2, and is essential for maintaining the stem cell fate of mitotic germ line nuclei. A STAT/KH domain containing RNA binding protein, GLD-1, is expressed in the pachytene zone of germ line and is required to restrict germ line mitosis and GLP-1 expression to the distal tip region of the gonad. Examinations done by Marin V. A. et al. implicated that a 34-nucleotide region of the *glp-1* 3' UTR contains two regulatory elements, and one of those is an element that represses *glp-1* translation in germ line. They further demonstrated that the STAT/KH domain protein GLD-1 binds directly and specifically to this repressor element and GLD-1 is required for GLP-1 repression in germ line. In the case of null *gld-1* allele, *q485*, meiotic germ line nuclei re-enter mitotic cell cycle in the proximal region of the gonad and resume the ability to proliferate, forming the germ line tumor. These over-generated germ line nuclei eventually break out from the gonad and kill the animal early in adult life.

Recent studies done by Pinkston J. M. et al. suggested that an insulin-receptor mutant *daf-2* is able to extend the life span of *gld-1(q485)* mutant animals by preventing cell proliferation and promoting apoptosis. DAF-2 is the *C. elegans* insulin/IGF receptor orthology, and its activity is required for numerous essential development processes in *C. elegans*. DAF-2 signals through a

conserved PI 3-kinase pathway. *daf-2* mutations that inhibit insulin/IGF signaling increase longevity in *C. elegans*. When these mutations are present in *gld-1(q485)* tumor background, these animals increase longevity and the tumor phenotype is less severe.

Human FLI-1, binding with a G-actin monomer, is a component of a transcriptional coactivator complex that acts with a nuclear hormone receptor. We reported that *C. elegans* full-length *fli-1::gfp* was detected in the area associated with the nucleus. These data suggest that *C. elegans* FLI-1 may play a role in regulating gene expression. As discussed in Chapter II, *C. elegans* FLI-1 interacts with LET-60 Ras in regulating gemline morphogenesis. *C. elegnas* LET-60 Ras in germ line control several development aspects, including the development transition of meiotic germ line nuclei from pachytene to diakinesis. In addition, *fli-1(ky535)* mutants exhibit increased number of germ line nuclei undergoing apoptosis at the flexure of the gonad. In this study, we asked whether *fli-1* mutations have effects on the tumor phenotype generated by *gld-1(q485)* null allele.

4. 3. Materials and Methods

***C. elegans* strains and genetics.** *C. elegans* were cultured as described. All experiments were done at 20°C unless otherwise noted. The Bristol strain N2 was used as the wild-type. The following mutations and transgenes were used. LGI: *gld-1(q485)* LGIII: *fli-1(ky535).*

DAPI staining of dissected gonads. The gonads of differently aged hermaphrodite animals were dissected and fixed with 3% paraformaldehyde containing 0.1M K_2HPO_4, pH7.2, for 1 hour at room temperature. The specimens were washed once with phosphate-buffered saline (PBS) with 0.1% Tween-20 (PBT) for 5 minutes followed by treatment with 100% methanol for 5 minute at -20°C. Specimens were treated with PBS containing 100ng/ml 4',6-diamidino-2-phenylindole (DAPI) for 10 minutes at room temperature followed by three washes in PBT. Gonads were mounted on a 2% agarose pad in M9 buffer with 1mg/ml 1,4-diazabicyclo[2.2.2]octane (DABCO) antifade reagent.

Analyze life spans. 10 adult animals were picked onto a single seeded NGM plate and let them lay eggs for 2 hrs. Adult animals were removed after laying eggs, the eggs on the plate were considered as animals with the same age. Synchronized animals were transferred onto a new plate with food each day and the number of animals was tracked from 1-day adult to determine the adult life span of each animal. The adult life span was used here because the germ line tumor phenotype was visible since 1-day adult.

Feeding RNAi. Vector 3F08 that produce *gld-1* hairpin sequence to induce RNAi was generously provided by Dr. Lisa Timmons. Bacteria Strain HT115

containing vector 3F08 were cultured in LB/TET (tetracycline)/AMP (ampicillin) at 37°C overnight. 2ml overnight culture was transferred into 20ml LB/TET/AMP and was incubated at 37°C for 1~4 hours until OD (595) = 0.4~0.8. 20 μL IPTG, 20 μL TET and 20 μL AMP were added to the culture. The bacteria culture were induced for 1~2 hrs at 37°C with shaking. NGM plates containing TET AMP IPTG were used to seed the bacteria. Before seeding the plates, additional 20 μL IPTG, 20 μL TET and 20 μL AMP were added to the plates. Each plate was seeded with 500 μL bacteria culture (bacteria were spread uniformly on the plate). The plates were air dried overnight.

10 synchronized L1 animals were picked on each plate seeded with RNAi food to make sure they were fed with enough food. Synchronized animals were checked of germ line tumor phenotype at different ages under DIC.

4. 4. Results

***gld-1* RNAi generates germ line tumor in wild-type and *fli-1(ky535)* animals.** *C. elegans gld-1* gene encodes an RNA-binding, STAT/KH domain containing protein GLD-1. GLD-1 protein is expressed in germ line pachytene zone. This GLD-1 expression is required to restrict germ line mitosis to the distal tip region of gonad where Notch membrane receptor GLP-1 is expressed. GLP-1 protein functions to maintain the proliferating ability of germ line stem cell at the distal tip region of the gonad, however GLP-1 expression disappears as germ line nuclei enter meiosis pachytene, where GLD-1 expression appears up and maintain the pachytene zone. GLD-1 is expressed throughout the pachytene zone until reach the flexure of the gonad where germ line nuclei exit pachytene and enter diakinesis and oogenesis begins. It has been shown that GLD-1 represses GLP-1 expression by binding to a repressor element located in *glp-1* 3' UTR. *gld-1(q485)* is a null mutation. With the loss of GLD-1 expression, GLP-1 is expressed throughout the gonad and allows the pachytene germ line nuclei re-enter mitosis and over proliferate. As a consequence of this over-proliferation, no oocyte is generated and mitotic germ line nuclei fill the gonad and produce a germ line tumor phenotype (Figure 4.1A). To examine how *fli-1* interacts with *gld-1*, *gld-1* RNAi was performed on both wild-type and *fli-1(ky535)* animals. Wild-type animals feeding on *gld-1* RNAi food displayed the germ line tumor phenotype, and this tumor phenotype became more severe day after day. *fli-1(ky535)* animals with *gld-1* RNAi also exhibited germ line tumor phenotype, which got more severe day after day. However, this was slightly less severe than the *gld-1* RNAi

done in wild-type background. The germ line nuclei of *fli-1(ky535)* animals with *gld-1* RNAi were larger in size and fewer in number than the germ line nuclei of wild-type animals with *gld-1* RNAi.

***fli-1(ky535)* mutation reduces the number of germ line nuclei in *gld-1(q485)* mutant and slight increases the life span of *gld-1(q485)* animals.** In order to more precisely analyze the severity of *gld-1* germ line tumor with or without the presence of *fli-1* mutant, *fli-1(ky535);gld-1(q485)* doubles were analyzed. *gld-1(q485); fli-1(ky535)* double mutants also exhibited germ line tumor phenotype (Figure 4.1B). However, compared with *gld-1(q485)* single mutant germ line tumor, the germ line nuclei in *gld-1(485); fli-1(ky535)* gonad were slightly larger and fewer in number (Figure 4.1). DAPI staining was used to visualize the germ line nuclei. By comparing the same aged animals, less germ line nuclei were observed in *gld-1(q485); fli-1(k535)* double-mutant animals than in *gld-1(q485)* single mutant animals (Figure 4.2).

To exam the possibility that *fli-1(ky535)* mutation extend the life span of *gld-1(q485)* animals by repressing the tumor phenotype, the adult life span of *gld-1(q485)* and *gld-1(q485); fli-1(ky535)* mutants was counted. As expected, as *fli-1(ky535)* reduced the number of germ line nuclei of *gld-1(q485)* animals, it also increased the adult life span of *gld-1(q485)* mutants (Figure 4.3). However, since feeding defects were observed in *fli-1(ky535)* animals, it is possible that slower metabolism makes *fli-1(ky535)* animals live longer than normal and therefore increases life span of *gld-1(q485); fli-1(ky535)* animals. In order to distinguish these two possibilities, the life span of *fli-1(ky535)* animals was compared with wild-type animals. Surprisingly, *fli-1(ky535)* mutation itself did not exhibit a

longer life span than wild-type animals (Figure 4.4). Some wild-type animals even lived slightly longer than *fli-1(ky535)* mutants. These data indicate that *fli-1(ky535)* mutation slightly represses the germ line tumor phenotype of *gld-1(q485)* animals. By doing so, animals carrying both *gld-1(q485)* and *fli-1(ky535)* mutations live slightly longer than *gld-1(q485)* single mutant animals.

***fli-1(ky535)* mutation increases apoptosis in *gld-1(q485)* animals.** A recent report from Pinkston et al. showed that mutations of insulin-receptor encoding gene *daf-2* increase the life span of *gld-1(q485)* animals by promoting apoptosis and repressing mitotic proliferation. Since a slightly increased life span was observed in *gld-1(q484); fli-1(ky535)* animals, the possibilities that *fli-1* mutation affects apoptosis and mitotic proliferation were examined. As germ line nuclei develop proximally, when they reach the flexure of gonad, some of them undergo apoptosis while the rest start oogenesis. In each gonad arm of 24-hour adult wild-type animals, on average 3.4±1.2 nuclei were detected undergoing apoptosis at the flexure region (Figure 2.10B), as assayed by GFP-tagged CED-1 in the somatic sheath cells of the gonad, a marker for engulfment of germ line nuclei. However, this number was dramatically increased in the gonads of *fli-1(ky535)* mutants, which was 8.0±1.8 nuclei (Figure 2.10C). The same GFP-tagged CED-1 was also used to examine the apoptosis rate in *gld-1(q485)* mutants and *gld-1(q485); fli-1(ky535)* mutants. It is already known that the apoptosis at the gonad flexure region is blocked in *gld-1* mutants. Consistent with this knowledge, a very low apoptosis rate was found in *gld-1(q485)* mutant gonads (0.23±0.6 nuclei were undergoing apoptosis) (Figure 4.5). In the case of *gld-*

1(q485); fli-1(ky535) mutants, on average, 0.87±1.06 nuclei were observed undergoing apoptosis (P=0.0022)(Figure 4.5). These observations suggest that *fli-1* mutation may have the ability to increase apoptosis in both wild-type background and *gld-1(q485)* mutant background.

***fli-1(ky535)* delays the re-entering of meiotic germ line nuclei into mitosis in *gld-1(q485)* animals.** Other reasonable hypotheses exist to explain the slight repression of *gld-1(q485)* tumor phenotype by *fli-1(ky535)* mutation. One such hypothesis is *fli-1(ky535)* may delay the meiotic germ line nuclei re-entering into mitosis. In *gld-1(q485)* mutant germ line, nuclei at the distal tip part of gonad are mitotic. Once they reach the transition zone, some nuclei leave mitosis and start meiosis. As germ line nuclei move out of the transition zone, all of them enter pachytene stage of meiosis and form a short pachytene zone before they re-enter mitosis at the proximal gonad (Figure 4.6A). For 24 hr old adult *gld-1(q485)* animals, the germ line pachytene zone spanned ~30 germ line nucleus rows in size. This pachytene zone became constricted as animals got older. In 48 hr old adult *gld-1(q485)* animals, this pachytene zone was only ~18 rows in size. For 96 hr old adult *gld-1(q485)* mutants, no pachytene zone or even transition zone existed and the germ line was filled with mitotic nuclei. Interestingly, when *fli-1(ky535)* mutation was present in *gld-1(q485)* animals, the pachytene zone was extended (Figure 4.6B). As for 24 hr old adult *gld-1(q485); fli-1(ky535)* double mutant animals, the pachytene zone was ~50 rows (compared to 30 rows in *gld-1(q485)* single mutants). The size of pachytene zone in this double mutant also became smaller when animals were older but less severe than *gld-1(q485)* single mutant. For 48 hr old adult *gld-1(q485); fli-1(ky535)* animals, the pachytene zone

was 26 rows. These preliminary data suggest that when *fli-1(ky535)* mutation is present in *gld-1(q485)* animals the germ line nuclei stay in pachytene stage longer and this may repress the tumor phenotype in *gld-1(q485)* mutation. Interestingly, in *gld-1(q485); fli-1(ky535)* double mutant germ line, many diakinesis stage germ line nuclei were detected in germ line pachytene zone, which were very rare in the *gld-1(q485)* mutant germ line. This single observation suggests that in *gld-1(q485);fli-1(ky535)* mutants, germ line nuclei need to enter diakinesis before re-enter mitosis, and this may delay the re-entry into mitosis and repress the tumor phenotype.

4. 5. Discussion

As discussed in Chapter II, FLI-1 regulates germ line morphogenesis and the coordination of germ line nuclei meiotic differentiation and rachis organization. The data reported here suggest that FLI-1 may also affect germ line tumor formation in *gld-1* mutant animals.

***fli-1(ky535)* mutant represses germ line tumor phenotype in *gld-1(q485)* animals by increasing apoptosis.** In *gld-1(q485)* mutants, instead of beginning oogenesis, pachytene stage germ line nuclei re-enter mitosis at the proximal part of the gonad. These proliferating mitotic nuclei generate numerous germ line nuclei that fill the entire gonad and form germ line tumor. Normally, some of the germ line nuclei undergo apoptosis at the flexure of the gonad, leaving the rest of germ line nuclei to start oogenesis. However, in *gld-1(q485)* mutants, this apoptosis pathway has been blocked. Since no germ line nuclei get into apoptosis, this mechanism may also contributes to the formation and severity of germ line tumor in *gld-1(ky535)* animals. *fli-1(ky535)* mutation itself increased the number of germ line nuclei undergoing apoptosis at the flexure of the gonad. When *fli-1(ky535)* was present in *gld-1(q485)* animals, the blockage of apoptosis pathway was somehow removed and a small portion of germ line nuclei started dying. The molecular mechanism of *fli-1(ky535)* in apoptosis is not known.

***fli-1(ky535)* may suppress the germ line tumor phenotype of *gld-1(q485)* by extending the germ line pachytene zone.** Our preliminary observations showed that in *gld-1(q485); fli-1(ky535)* double mutants the germ line pachytene zone was longer than in *gld-1(q485)* single mutant animals. This

indicates that *fli-1(ky535)* mutation has the ability to maintain the germ line nuclei at meiosis stage or delay re-entry into mitosis. How *fli-1(ky535)* mutation is able to do this is not known. Interestingly, in *gld-1(q485); fli-1(ky535)* double mutant germ line, many diakinesis stage germ line nuclei were detected in germ line pachytene zone, which were very rare in the *gld-1(q485)* mutant germ line. This observation leaves us interesting questions, such as whether in *gld-1(q485); fli-1(ky535)* mutant, the germ line pachytene nuclei are not allowed to re-enter mitosis until they further develop into diakinesis. It is also possible that FLI-1 regulates germ line proliferation directly.

Based on these preliminary data we observed, we suggest that *fli-1(ky535)* mutation represses the germ line tumor phenotype of *gld-1(q485)* mutation. However, it is also possible that *fli-1(ky535)* mutation may not represses the germ line tumor directly. Instead this repression we observed may due to slower metabolism of *fli-1(ky535)* mutation, which slows down every biological process including tumor generation. To distinguish these two possibilities, autonomy analysis is necessary. One way to perform this autonomy analysis is to do *fli-1* RNAi in *gld-1(q485); rrf-3* animals, which are somatic RNAi defective but germ line RNAi sensitive. If the same germ line tumor repression can be repeated in these animals by introducing *fli-1* dsRNA, it may provide strong evidence to support that *fli-1(ky535)* mutation represses germ line tumor phenotype directly. This experiment is now being designed. The study of interaction between *fli-1(ky535)* and *gld-1(q485)* is going to provide us more understandings about the molecular mechanisms of FLI-1 functions in *C. elegans* germ line.

Figure 4. 1

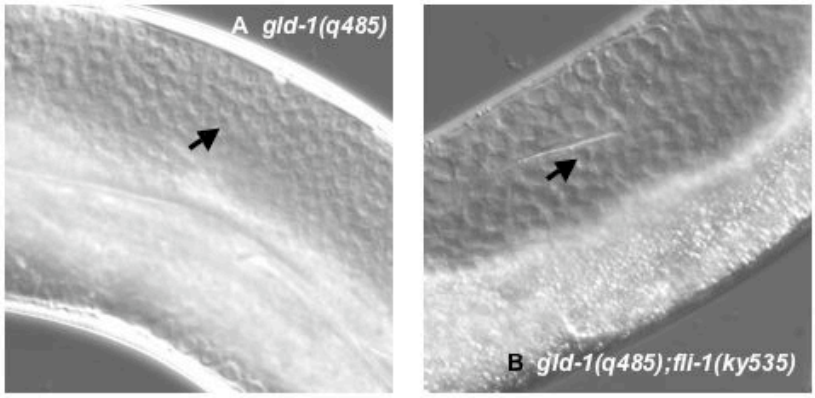

Figure 4. 1 *gld-1(q485)* mutants and *gld-1(q485); fli-1(ky535)* mutants display germ line tumor phenotype. Shown are DIC images of germ line tumor. Arrows point out germ line nuclei. (A) In *gld-1(q485)* mutants, meiotic germ line nuclei re-enter mitosis and gain the ability to proliferate. The excess mitosis nuclei fill the entire germ line and form a germ line tumor. (B) The germ line tumor also exists in *gld-1(q485); fli-1(ky535)* double mutant gonad, but the nuclei are larger and fewer in number, indicating fewer mitotic divisions. Numerous germ line nuclei occupy the entire germ line.

Figure 4. 2

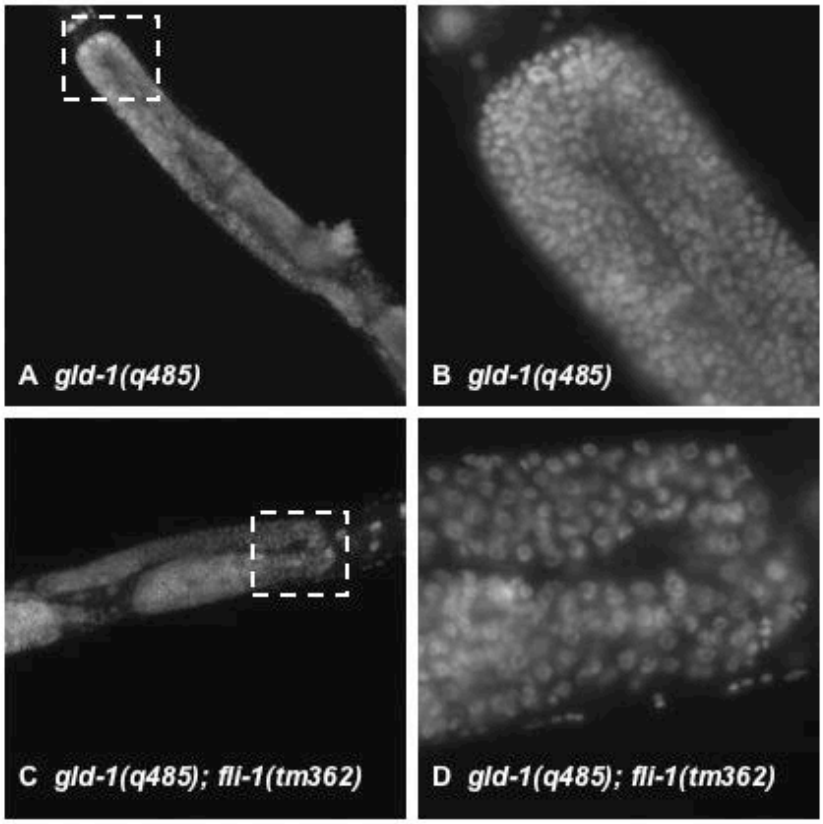
A gld-1(q485)
B gld-1(q485)
C gld-1(q485); fli-1(tm362)
D gld-1(q485); fli-1(tm362)

Figure 4. 2 Synchronized *gld-1(q485); fli-1(ky535)* double mutants contain less germ line nuclei than *gld-1(q485)* single mutant animals. Shown are pictures of DAPI stained 24 hr old adult animals. (B) is enlarged picture from the dotted line of (A), and (D) is the enlarged picture from the dotted line of (C). (A), (C) are at the same magnification, and (B) and (D) are at the same magnification as well. Comparing the flexure region of *gld-1(q485)* and *gld-1(q485); fli-1(ky535)*, germ line nuclei are appeared to be larger and fewer in *gld-1(q485); fli-1(ky535)* double mutant (D) than in *gld-1(q485)* single mutant (B).

Figure 4.3

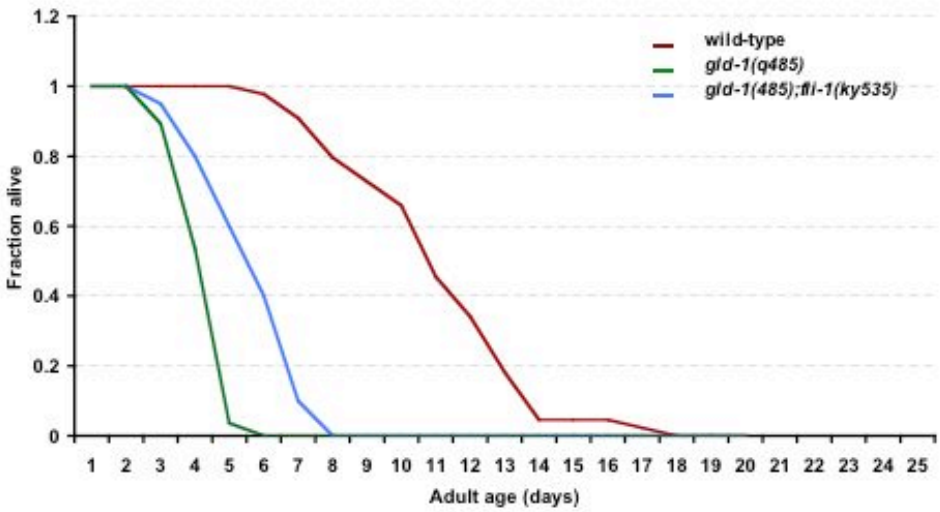
wild-type
gld-1(q485)
gld-1(485);fli-1(ky535)
Fraction alive
1.2
1
0.8
0.6
0.4
0.2
0
1 2 3 4 5 6 7 8 9 10 11 12 13 14 15 16 17 18 19 20 21 22 23 24 25
Adult age (days)

Figure 4. 3 *fli-1(ky535)* mutation delays the death of *gld-1(q485)* mutant caused by forming germ line tumor. Different mutant animals were grown in parallel and the days of adult animal lived were counted (Living animals were able to move when they were touched by the tip of worm picker, however dead animals did not move when they were touched.). x axis represents the age of animals in adult days, and y axis indicates the fraction of animals that were still alive at the corresponding adult age. *gld-1(q485)* animals had a much shorter life span than wild-type animals. When *fli-1(ky535)* mutation was present in *gld-1(q485)* background, this *fli-1(ky535)* mutation slightly suppressed the lethality caused by *gld-1(q485)* germ line tumor.

Figure 4. 4

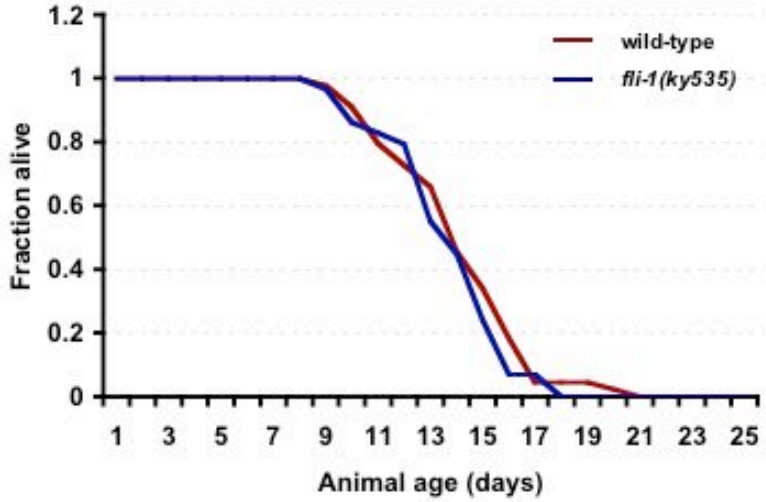
wild-type
fli-1(ky535)
Fraction alive
1.2
1
0.8
0.6
0.4
0.2
0
1 3 5 7 9 11 13 15 17 19 21 23 25
Animal age (days)

Figure 4. 4 *fli-1(ky535)* mutation alone does not affect life span. To address whether *fli-1(ky535)* mutation itself makes animals live longer, the life spans of *fli-1(ky535)* mutants were compared with wild-type animals. It turns out that *fli-1(ky535)* mutants exhibited similar life span as wild-type animals.

Figure 4. 5

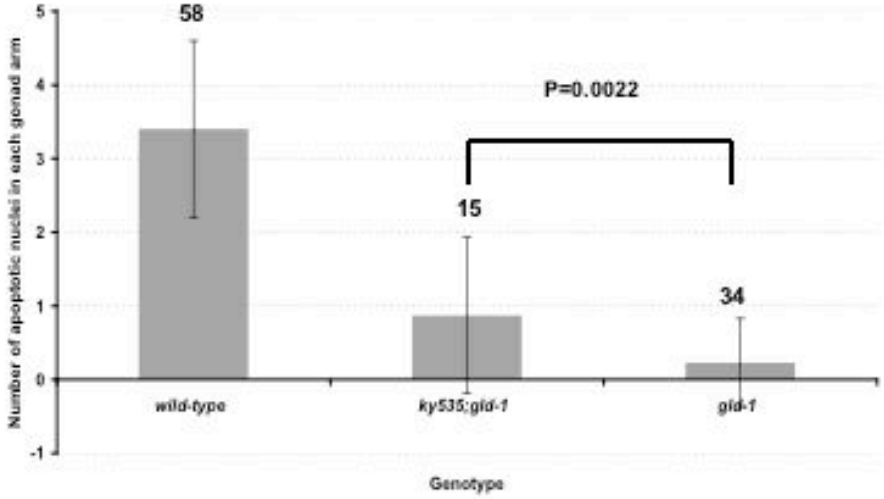
58
P=0.0022
15
34
Number of apoptotic nuclei in each gonad arm
5
4
3
2
1
0
-1
wild-type
ky535;gld-1
gld-1
Genotype

Figure 4. 5 *fli-1(ky535)* mutation partially restores germ line apoptosis in *gld-1(q485)* mutants. The germ line nuclei that were undergoing programmed cell death were visualized by GFP-tagged CED-1. The bars show the numbers of germ line nuclei that were doing apoptosis in different mutants. x axis represents genotype, and y axis shows the number of apoptotic germ line nuclei. Error bars are standard deviation. “n” numbers are labeled on the top of each bar.

Figure 4. 6

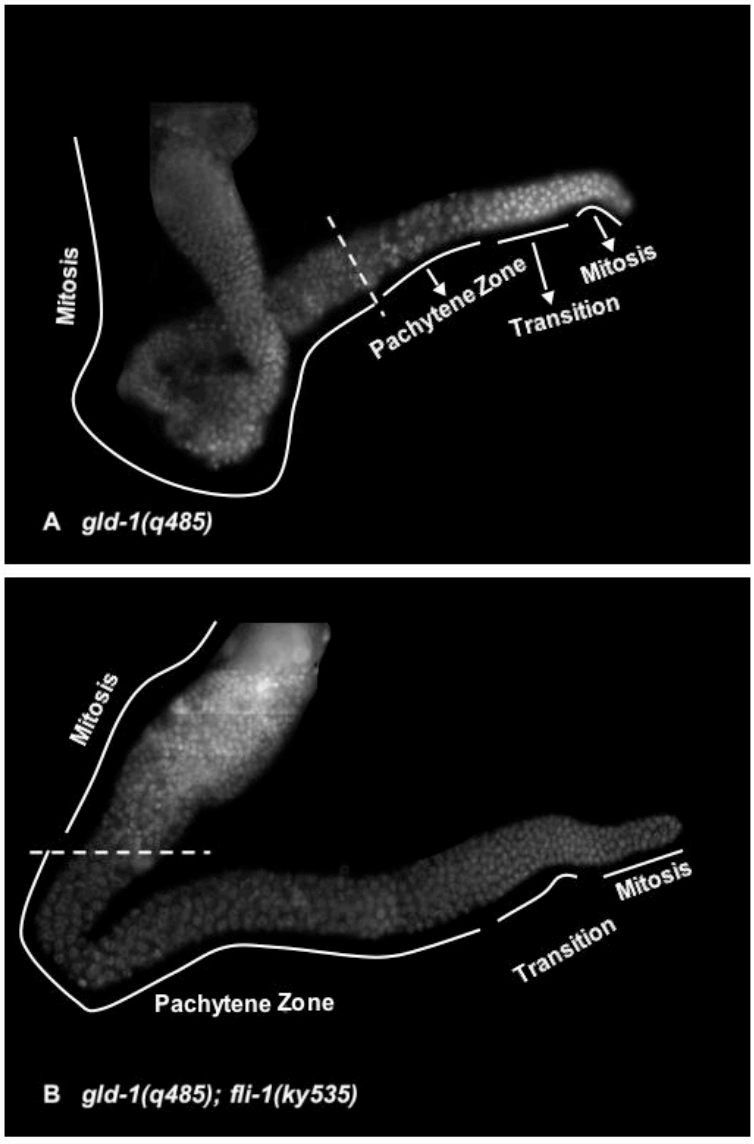
Mitosis
Pachytene Zone
Transition
Mitosis
A gld-1(q485)
Mitosis
Mitosis
Transition
Pachytene Zone
B gld-1(q485); fli-1(ky535)

Figure 4. 6 *fli-1(ky535)* mutation delays the meiotic germ line nuclei re-entering into mitosis in *gld-1(q485)* mutants. Dissected gonads were stained with DAPI. Dotted lines divide pachytene zone and the mitosis zone formed by nuclei re-entered mitosis. In *gld-1(q485)* mutants, after germ line nuclei came out of transition zone, germ line nuclei entered pachytene stage and formed a short pachytene zone (A). For *gld-1(q485); fli-1(ky535)* double mutant animals, more germ line nuclei stayed in pachytene stage and formed a much longer pachytene zone (B) than in *gld-1(q485)* mutants.

References:

1. Ahnn, J. and Fire, A. (1994). A screen for genetic loci required for body-wall muscle development during embryogenesis in Caenorhabditis elegans. *Genetics* **137**, 483-98.

2. Aroian, R. V., Koga, M., Mendel, J. E., Ohshima, Y. and Sternberg, P. W. (1990). The let-23 gene necessary for Caenorhabditis elegans vulval induction encodes a tyrosine kinase of the EGF receptor subfamily. *Nature* **348**, 693-9.

3. Asch, H. L., Head, K., Dong, Y., Natoli, F., Winston, J. S., Connolly, J. L. and Asch, B. B. (1996). Widespread loss of gelsolin in breast cancers of humans, mice, and rats. *Cancer Res* **56**, 4841-5.

4. Austin, J. and Kimble, J. (1987). glp-1 is required in the germ line for regulation of the decision between mitosis and meiosis in C. elegans. *Cell* **51**, 589-99.

5. Beitel, G. J., Clark, S. G. and Horvitz, H. R. (1990). Caenorhabditis elegans ras gene let-60 acts as a switch in the pathway of vulval induction. *Nature* **348**, 503-9.

6. Beitel, G. J., Tuck, S., Greenwald, I. and Horvitz, H. R. (1995). The Caenorhabditis elegans gene lin-1 encodes an ETS-domain protein and defines a branch of the vulval induction pathway. *Genes Dev* **9**, 3149-62.

7. Berry, L. W., Westlund, B. and Schedl, T. (1997). Germ-line tumor formation caused by activation of glp-1, a Caenorhabditis elegans member of the Notch family of receptors. *Development* **124**, 925-36.

8. Biegel, J. A., Janss, A. J., Raffel, C., Sutton, L., Rorke, L. B., Harper, J. M. and Phillips, P. C. (1997). Prognostic significance of chromosome 17p deletions

in childhood primitive neuroectodermal tumors (medulloblastomas) of the central nervous system. *Clin Cancer Res* **3**, 473-8.

9. Campbell, H. D., Fountain, S., McLennan, I. S., Berven, L. A., Crouch, M. F., Davy, D. A., Hooper, J. A., Waterford, K., Chen, K. S., Lupski, J. R. et al. (2002). Fliih, a gelsolin-related cytoskeletal regulator essential for early mammalian embryonic development. *Mol Cell Biol* **22**, 3518-26.

10. Campbell, H. D., Fountain, S., Young, I. G., Claudianos, C., Hoheisel, J. D., Chen, K. S. and Lupski, J. R. (1997). Genomic structure, evolution, and expression of human FLII, a gelsolin and leucine-rich-repeat family member: overlap with LLGL. *Genomics* **42**, 46-54.

11. Campbell, H. D., Schimansky, T., Claudianos, C., Ozsarac, N., Kasprzak, A. B., Cotsell, J. N., Young, I. G., de Couet, H. G. and Miklos, G. L. (1993). The Drosophila melanogaster flightless-I gene involved in gastrulation and muscle degeneration encodes gelsolin-like and leucine-rich repeat domains and is conserved in Caenorhabditis elegans and humans. *Proc Natl Acad Sci U S A* **90**, 11386-90.

12. Chang, C., Hopper, N. A. and Sternberg, P. W. (2000). Caenorhabditis elegans SOS-1 is necessary for multiple RAS-mediated developmental signals. *Embo J* **19**, 3283-94.

13. Chen, K. S., Gunaratne, P. H., Hoheisel, J. D., Young, I. G., Miklos, G. L., Greenberg, F., Shaffer, L. G., Campbell, H. D. and Lupski, J. R. (1995). The human homologue of the Drosophila melanogaster flightless-I gene (flil) maps within the Smith-Magenis microdeletion critical region in 17p11.2. *Am J Hum Genet* **56**, 175-82.

14. Church, D. L., Guan, K. L. and Lambie, E. J. (1995). Three genes of the MAP kinase cascade, mek-2, mpk-1/sur-1 and let-60 ras, are required for meiotic cell cycle progression in Caenorhabditis elegans. *Development* **121**, 2525-35.

15. Clark, S. G., Stern, M. J. and Horvitz, H. R. (1992). C. elegans cell-signalling gene sem-5 encodes a protein with SH2 and SH3 domains. *Nature* **356**, 340-4.

16. Cripps, R. M., Ball, E., Stark, M., Lawn, A. and Sparrow, J. C. (1994). Recovery of dominant, autosomal flightless mutants of Drosophila melanogaster and identification of a new gene required for normal muscle structure and function. *Genetics* **137**, 151-64.

17. Crittenden, S. L., Eckmann, C. R., Wang, L., Bernstein, D. S., Wickens, M. and Kimble, J. (2003). Regulation of the mitosis/meiosis decision in the Caenorhabditis elegans germline. *Philos Trans R Soc Lond B Biol Sci* **358**, 1359-62.

18. Crittenden, S. L., Leonhard, K. A., Byrd, D. T. and Kimble, J. (2006). Cellular analyses of the mitotic region in the Caenorhabditis elegans adult germ line. *Mol Biol Cell* **17**, 3051-61.

19. Davy, D. A., Campbell, H. D., Fountain, S., de Jong, D. and Crouch, M. F. (2001). The flightless I protein colocalizes with actin- and microtubule-based structures in motile Swiss 3T3 fibroblasts: evidence for the involvement of PI 3-kinase and Ras-related small GTPases. *J Cell Sci* **114**, 549-62.

20. Deak, II, Bellamy, P. R., Bienz, M., Dubuis, Y., Fenner, E., Gollin, M., Rahmi, A., Ramp, T., Reinhardt, C. A. and Cotton, B. (1982). Mutations affecting the indirect flight muscles of Drosophila melanogaster. *J Embryol Exp*

Morphol **69**, 61-81.

21. Dentler, W. L. and Adams, C. (1992). Flagellar microtubule dynamics in Chlamydomonas: cytochalasin D induces periods of microtubule shortening and elongation; and colchicine induces disassembly of the distal, but not proximal, half of the flagellum. *J Cell Biol* **117**, 1289-98.

22. Eckmann, C. R., Crittenden, S. L., Suh, N. and Kimble, J. (2004). GLD-3 and control of the mitosis/meiosis decision in the germline of Caenorhabditis elegans. *Genetics* **168**, 147-60.

23. Fong, K. S. and de Couet, H. G. (1999). Novel proteins interacting with the leucine-rich repeat domain of human flightless-I identified by the yeast two-hybrid system. *Genomics* **58**, 146-57.

24. Francis, R., Barton, M. K., Kimble, J. and Schedl, T. (1995a). gld-1, a tumor suppressor gene required for oocyte development in Caenorhabditis elegans. *Genetics* **139**, 579-606.

25. Francis, R., Maine, E. and Schedl, T. (1995b). Analysis of the multiple roles of gld-1 in germline development: interactions with the sex determination cascade and the glp-1 signaling pathway. *Genetics* **139**, 607-30.

26. Goshima, M., Kariya, K., Yamawaki-Kataoka, Y., Okada, T., Shibatohge, M., Shima, F., Fujimoto, E. and Kataoka, T. (1999). Characterization of a novel Ras-binding protein Ce-FLI-1 comprising leucine-rich repeats and gelsolin-like domains. *Biochem Biophys Res Commun* **257**, 111-6.

27. Greenberg, F., Lewis, R. A., Potocki, L., Glaze, D., Parke, J., Killian, J., Murphy, M. A., Williamson, D., Brown, F., Dutton, R. et al. (1996). Multi-disciplinary clinical study of Smith-Magenis syndrome (deletion 17p11.2). *Am J*

Med Genet **62**, 247-54.

28. Gumienny, T. L., Lambie, E., Hartwieg, E., Horvitz, H. R. and Hengartner, M. O. (1999). Genetic control of programmed cell death in the Caenorhabditis elegans hermaphrodite germline. *Development* **126**, 1011-22.

29. Hall, D. H. (1995). Electron microscopy and three-dimensional image reconstruction. *Methods Cell Biol* **48**, 395-436.

30. Hall, D. H., Winfrey, V. P., Blaeuer, G., Hoffman, L. H., Furuta, T., Rose, K. L., Hobert, O. and Greenstein, D. (1999). Ultrastructural features of the adult hermaphrodite gonad of Caenorhabditis elegans: relations between the germ line and soma. *Dev Biol* **212**, 101-23.

31. Han, M., Golden, A., Han, Y. and Sternberg, P. W. (1993). C. elegans lin-45 raf gene participates in let-60 ras-stimulated vulval differentiation. *Nature* **363**, 133-40.

32. Han, M. and Sternberg, P. W. (1990). let-60, a gene that specifies cell fates during C. elegans vulval induction, encodes a ras protein. *Cell* **63**, 921-31.

33. Han, M. and Sternberg, P. W. (1991). Analysis of dominant-negative mutations of the Caenorhabditis elegans let-60 ras gene. *Genes Dev* **5**, 2188-98.

34. Hansen, D., Hubbard, E. J. and Schedl, T. (2004a). Multi-pathway control of the proliferation versus meiotic development decision in the Caenorhabditis elegans germline. *Dev Biol* **268**, 342-57.

35. Hansen, D., Wilson-Berry, L., Dang, T. and Schedl, T. (2004b). Control of the proliferation versus meiotic development decision in the C. elegans germline through regulation of GLD-1 protein accumulation. *Development* **131**, 93-104.

36. Henderson, S. T., Gao, D., Lambie, E. J. and Kimble, J. (1994). lag-2 may

encode a signaling ligand for the GLP-1 and LIN-12 receptors of C. elegans. *Development* **120**, 2913-24.

37. Hill, R. J. and Sternberg, P. W. (1992). The gene lin-3 encodes an inductive signal for vulval development in C. elegans. *Nature* **358**, 470-6.

38. Hirsh, D., Oppenheim, D. and Klass, M. (1976). Development of the reproductive system of Caenorhabditis elegans. *Dev Biol* **49**, 200-19.

39. Homyk, T. and Sheppard, D. E. (1977). Behavioral Mutants of DROSOPHILA MELANOGASTER. I. Isolation and Mapping of Mutations Which Decrease Flight Ability. *Genetics* **87**, 95-104.

40. Jones, A. R., Francis, R. and Schedl, T. (1996). GLD-1, a cytoplasmic protein essential for oocyte differentiation, shows stage- and sex-specific expression during Caenorhabditis elegans germline development. *Dev Biol* **180**, 165-83.

41. Kadyk, L. C. and Kimble, J. (1998). Genetic regulation of entry into meiosis in Caenorhabditis elegans. *Development* **125**, 1803-13.

42. Kelly, W. G., Xu, S., Montgomery, M. K. and Fire, A. (1997). Distinct requirements for somatic and germline expression of a generally expressed Caernorhabditis elegans gene. *Genetics* **146**, 227-38.

43. Kimble, J. and Simpson, P. (1997). The LIN-12/Notch signaling pathway and its regulation. *Annu Rev Cell Dev Biol* **13**, 333-61.

44. Kimble, J. E. and White, J. G. (1981). On the control of germ cell development in Caenorhabditis elegans. *Dev Biol* **81**, 208-19.

45. Koana, T. and Hotta, Y. (1978). Isolation and characterization of flightless mutants in Drosophila melanogaster. *J Embryol Exp Morphol* **45**, 123-43.

46. Kwiatkowski, D. J. (1999). Functions of gelsolin: motility, signaling, apoptosis, cancer. *Curr Opin Cell Biol* **11**, 103-8.

47. Lackner, M. R., Kornfeld, K., Miller, L. M., Horvitz, H. R. and Kim, S. K. (1994). A MAP kinase homolog, mpk-1, is involved in ras-mediated induction of vulval cell fates in Caenorhabditis elegans. *Genes Dev* **8**, 160-73.

48. Lee, Y. H., Campbell, H. D. and Stallcup, M. R. (2004). Developmentally essential protein flightless I is a nuclear receptor coactivator with actin binding activity. *Mol Cell Biol* **24**, 2103-17.

49. Lee, Y. H. and Stallcup, M. R. (2006). Interplay of Fli-I and FLAP1 for regulation of beta-catenin dependent transcription. *Nucleic Acids Res* **34**, 5052-9.

50. Liu, Y. T. and Yin, H. L. (1998). Identification of the binding partners for flightless I, A novel protein bridging the leucine-rich repeat and the gelsolin superfamilies. *J Biol Chem* **273**, 7920-7.

51. Lundquist, E. A., Herman, R. K., Shaw, J. E. and Bargmann, C. I. (1998). UNC-115, a conserved protein with predicted LIM and actin-binding domains, mediates axon guidance in C. elegans. *Neuron* **21**, 385-92.

52. Marin, V. A. and Evans, T. C. (2003). Translational repression of a C. elegans Notch mRNA by the STAR/KH domain protein GLD-1. *Development* **130**, 2623-32.

53. Mello, C. and Fire, A. (1995). DNA transformation. *Methods Cell Biol* **48**, 451-82.

54. Miklos, G. L. and De Couet, H. G. (1990). The mutations previously designated as flightless-I3, flightless-O2 and standby are members of the W-2 lethal complementation group at the base of the X-chromosome of Drosophila

melanogaster. *J Neurogenet* **6**, 133-51.

55. Miller, L. M., Gallegos, M. E., Morisseau, B. A. and Kim, S. K. (1993). lin-31, a Caenorhabditis elegans HNF-3/fork head transcription factor homolog, specifies three alternative cell fates in vulval development. *Genes Dev* **7**, 933-47.

56. Mootz, D., Ho, D. M. and Hunter, C. P. (2004). The STAR/Maxi-KH domain protein GLD-1 mediates a developmental switch in the translational control of C. elegans PAL-1. *Development* **131**, 3263-72.

57. Nilsson, L., Li, X., Tiensuu, T., Auty, R., Greenwald, I. and Tuck, S. (1998). Caenorhabditis elegans lin-25: cellular focus, protein expression and requirement for sur-2 during induction of vulval fates. *Development* **125**, 4809-19.

58. Ohmachi, M., Rocheleau, C. E., Church, D., Lambie, E., Schedl, T. and Sundaram, M. V. (2002). C. elegans ksr-1 and ksr-2 have both unique and redundant functions and are required for MPK-1 ERK phosphorylation. *Curr Biol* **12**, 427-33.

59. Pepper, A. S., Killian, D. J. and Hubbard, E. J. (2003). Genetic analysis of Caenorhabditis elegans glp-1 mutants suggests receptor interaction or competition. *Genetics* **163**, 115-32.

60. Pinkston, J. M., Garigan, D., Hansen, M. and Kenyon, C. (2006). Mutations that increase the life span of C. elegans inhibit tumor growth. *Science* **313**, 971-5.

61. Schedl, T. (1997). Developmental genetics of the Germ Line. In *C. elegans II*, (ed. D. Riddle T. Blumethal B. J. Meyer and J. R. Priess). Cold Spring Harbor, NY: Cold Spring Harbor Laboratory Press.

62. Scheurlen, W. G., Seranski, P., Mincheva, A., Kuhl, J., Sorensen, N.,

Krauss, J., Lichter, P., Poustka, A. and Wilgenbus, K. K. (1997). High-resolution deletion mapping of chromosome arm 17p in childhood primitive neuroectodermal tumors reveals a common chromosomal disruption within the Smith-Magenis region, an unstable region in chromosome band 17p11.2. *Genes Chromosomes Cancer* **18**, 50-8.

63. Seranski, P., Heiss, N. S., Dhorne-Pollet, S., Radelof, U., Korn, B., Hennig, S., Backes, E., Schmidt, S., Wiemann, S., Schwarz, C. E. et al. (1999). Transcription mapping in a medulloblastoma breakpoint interval and Smith-Magenis syndrome candidate region: identification of 53 transcriptional units and new candidate genes. *Genomics* **56**, 1-11.

64. Singh, N. and Han, M. (1995). sur-2, a novel gene, functions late in the let-60 ras-mediated signaling pathway during Caenorhabditis elegans vulval induction. *Genes Dev* **9**, 2251-65.

65. Smith, A. C., McGavran, L., Robinson, J., Waldstein, G., Macfarlane, J., Zonona, J., Reiss, J., Lahr, M., Allen, L. and Magenis, E. (1986). Interstitial deletion of (17)(p11.2p11.2) in nine patients. *Am J Med Genet* **24**, 393-414.

66. Straub, K. L., Stella, M. C. and Leptin, M. (1996). The gelsolin-related flightless I protein is required for actin distribution during cellularisation in Drosophila. *J Cell Sci* **109 (Pt 1)**, 263-70.

67. Sulston, J. and Hodgkin, J. (1988). Methods. In *The Nematode Caenorhabditis elegans*, (ed. W. B. Wood), pp. 587-606. Cold Spring Harbor, New York: Cold Spring Harbor Laboratory Press.

68. Sundaram, M. and Han, M. (1995). The C. elegans ksr-1 gene encodes a novel Raf-related kinase involved in Ras-mediated signal transduction. *Cell* **83**,

889-901.

69. Tanaka, M., Sazawa, A., Shinohara, N., Kobayashi, Y., Fujioka, Y., Koyanagi, T. and Kuzumaki, N. (1999). Gelsolin gene therapy by retrovirus producer cells for human bladder cancer in nude mice. *Cancer Gene Ther* **6**, 482-7.

70. Timmons, L. (2006). Delivery methods for RNA interference in C. elegans. *Methods Mol Biol* **351**, 119-25.

71. Trask, B. J., Mefford, H., van den Engh, G., Massa, H. F., Juyal, R. C., Potocki, L., Finucane, B., Abuelo, D. N., Witt, D. R., Magenis, E. et al. (1996). Quantification by flow cytometry of chromosome-17 deletions in Smith-Magenis syndrome patients. *Hum Genet* **98**, 710-8.

72. White, J. G. (1988). The Anatomy. In *he Nematode Caenorhabditis elegans*, (ed. W. B. Wood). Cold Spring Harbor, NY: Cold Spring Harbor Laboratory Press.

73. Wilgenbus, K. K., Seranski, P., Brown, A., Leuchs, B., Mincheva, A., Lichter, P. and Poustka, A. (1997). Molecular characterization of a genetically unstable region containing the SMS critical area and a breakpoint cluster for human PNETs. *Genomics* **42**, 1-10.

74. Williams, B. D. and Waterston, R. H. (1994). Genes critical for muscle development and function in Caenorhabditis elegans identified through lethal mutations. *J Cell Biol* **124**, 475-90.

75. Wu, Y. and Han, M. (1994). Suppression of activated Let-60 ras protein defines a role of Caenorhabditis elegans Sur-1 MAP kinase in vulval differentiation. *Genes Dev* **8**, 147-59.

76. Zhou, Z., Hartwieg, E. and Horvitz, H. R. (2001). CED-1 is a

transmembrane receptor that mediates cell corpse engulfment in C. elegans. *Cell* **104**, 43-56.